1-Alkyl-8-(piperazine-1-sulfonyl)phenylxanthines: Development and Characterization of Adenosine A_{2B} Receptor Antagonists and a New Radioligand with Subnanomolar Affinity and Subtype Specificity

Thomas Borrmann, Sonja Hinz, Daniela C. G. Bertarelli, Wenjin Li, Nicole C. Florin, Anja B. Scheiff, and Christa E. Müller*

PharmaCenter Bonn, Pharmaceutical Institute, Pharmaceutical Chemistry I, An der Immenburg 4, D-53121 Bonn, Germany

Received March 31, 2009

A new series of 1-alkyl-8-(piperazine-1-sulfonyl)phenylxanthines was designed, synthesized, and characterized in radioligand binding and functional assays at A_{2B} adenosine receptors. A_{2B} antagonists with subnanomolar affinity and high selectivity were discovered. The most potent compounds were 1-ethyl-8-(4-(4-(4-trifluoromethylbenzyl)piperazine-1-sulfonyl)phenyl)xanthine (**24**, PSB-09120, K_i (human A_{2B}) = 0.157 nM) and 8-(4-(4-(4-chlorobenzyl)piperazine-1-sulfonyl)phenyl)-1-propylxanthine (**17**, PSB-0788, K_i (human A_{2B}) = 0.393 nM). Moreover, 8-(4-(4-(4-chlorophenyl)piperazine-1-sulfonyl)phenyl)-1-propylxanthine (**35**, PSB-603) was developed as an A_{2B}-specific antagonist exhibiting a K_i value of 0.553 nM at the human A_{2B} receptor and virtually no affinity for the human and rat A_1 and A_{2A} and the human A_3 receptors up to a concentration of 10 μM. A tritiated form of the compound was prepared as a new radioligand and characterized in kinetic, saturation, and competition studies. It was shown to be a useful pharmacological tool for the selective labeling of human as well as rodent A_{2B} receptors (K_D human A_{2B} 0.403 nM, mouse A_{2B} 0.351 nM).

Downloaded by UNIV OF NEWCASTLE on October 11, 2009 | http://pubs.acs.org
Publication Date (Web): May 27, 2009 | doi: 10.1021/jm900413e

Introduction

Adenosine is an endogenous purine nucleoside activating four subtypes of G protein-coupled receptors (adenosine receptors, AdoR) that have been cloned and termed A_1, A_{2A}, A_{2B}, and A_3.[1] Adenosine induces bronchoconstriction in asthmatics,[2] and the exhaled breath condensate[3] and bronchoalveolar lavage fluid[4] of asthmatic patients contains increased concentrations of adenosine. Studies with adenosine deaminase (ADA[a])-deficient mice revealed a causal connection between increased lung adenosine levels and a phenotype of pulmonary inflammation.[5,6] These findings strongly suggested that adenosine plays an important role in the pathophysiology of chronic inflammatory lung diseases.

The A_{2B}AdoR is a low affinity receptor that is thought to remain silent under physiological conditions and to be activated in consequence of increased extracellular adenosine levels.[7,8] It is mainly expressed in the gastrointestinal tract, bladder, lung, and on mast cells.[1,9] Activation of A_{2B}AdoR can stimulate adenylate cyclase and phospholipase C through activation of G_s and G_q proteins, respectively. Coupling to mitogen-activated protein kinases has also been described.[10]

There is ample evidence suggesting that the A_{2B}AdoR mediates proinflammatory effects in the lung.[11] Stimulation of human mast cells, which is pivotal to the pathophysiology of asthma, is potentiated by the activation of A_{2B}AdoR, releasing the inflammatory cytokines interleukin-4 (IL-4), IL-8, and IL-13.[10,12,13] A series of experiments described the A_{2B} receptor-mediated release of proinflammatory cytokines from a number of cells and tissues, including bronchial smooth muscle and epithelial cells, lung fibroblasts, and intestinal epithelial cells.[14−17] It was demonstrated that activation of the A_{2B}AdoR promotes the differentiation of human fibroblasts into myofibroblasts via IL-6 release,[16] resulting in airway remodeling, which is known to play an important role in the pathophysiology of inflammatory airway diseases.[18] A_{2B} antagonists proved to attenuate the release of IL-19 from human bronchial epithelial cells[15] and to abolish the secretion of IL-13 from mouse bone marrow-derived mast cells.[19]

In another set of experiments, it was observed that 5′-*N*-ethylcarboxamidoadenosine (NECA), a nonselective AdoR agonist, inhibited tumor necrosis factor alpha (TNF_α) release in mouse peritoneal macrophages of A_{2A}AdoR knockout mice, an effect that could be blocked by the A_{2B}AdoR antagonist MRS-1754 (**8**).[20] Yang et al. reported that A_{2B}AdoR knockout mice developed low-grade inflammation due to increases in IL-6 and TNF_α.[21] Both studies suggested that, in addition to the predominant A_{2A}-mediated anti-inflammatory effect of adenosine, activation of A_{2B}AdoR might also lead to a reduction of inflammation.

However, follow-up experiments with A_{2B}AdoR knockout and wild-type mice and with mouse peritoneal macrophages, isolated from A_{2B}AdoR knockout and wild-type mice, demonstrated that NECA induced a release of the proinflammatory cytokine IL-6 in wild-type mice, which was abrogated by A_{2B}AdoR antagonists or by genetic ablation of A_{2B}AdoR. In this study, it could also be shown that the NECA-induced suppression of TNF_α in mouse peritoneal macrophages observed by Kreckler et al.[20] was neither affected by A_{2B} antagonists nor by genetic ablation of A_{2B}AdoR.[22] These results indicated that activation of A_{2B}AdoR by adenosine might not contribute significantly to the primarily A_{2A}-mediated suppression of TNF_α release.[23,24]

* To whom correspondence should be addressed: Phone: +49-228-73-2301. Fax: +49-228-73-2567. E-mail: christa.mueller@uni-bonn.de.

[a] Abbreviations ADA, adenosine deaminase; AdoR, adenosine receptor; CADO, 2-chloroadenosine; [^{3}H]CCPA, [^{3}H]2-chloro-N^6-cyclopentyladenosine; CHO cells, Chinese hamster ovary cells; DPCPX, 8-cyclopentyl-1,3-dipropylxanthine; DSS, dextran sodium sulfate; EDC, *N*-(3-(dimethylamino)propyl)-*N*′-ethylcarbodiimide; HMDS, 1,1,1,3,3,3-hexamethyldisilazane; [^{125}I]I-ABOPX, [^{125}I]3-(4-amino-3-iodobenzyl)-8-phenyl-(4-oxyacetic acid)-1-propylxanthine; IL, interleukin; NECA, 5′-*N*-ethylcarboxamidoadenosine; PPSE, polyphosphoric acid trimethylsilyl ester; PSA, polar surface area; PSB, Pharmaceutical Sciences Bonn; TNBS, 2,4,6-trinitrobenzene sulfonic acid; TNF_α, tumor necrosis factor alpha; VEGF, vascular endothelial growth factor.

10.1021/jm900413e CCC: $40.75 © 2009 American Chemical Society
Published on Web 05/27/2009

Chart 1. A_{2B} Antagonists and their K_i Values at AdoR Subtypes (h = Human, r = Rat)[9,27,40−47]

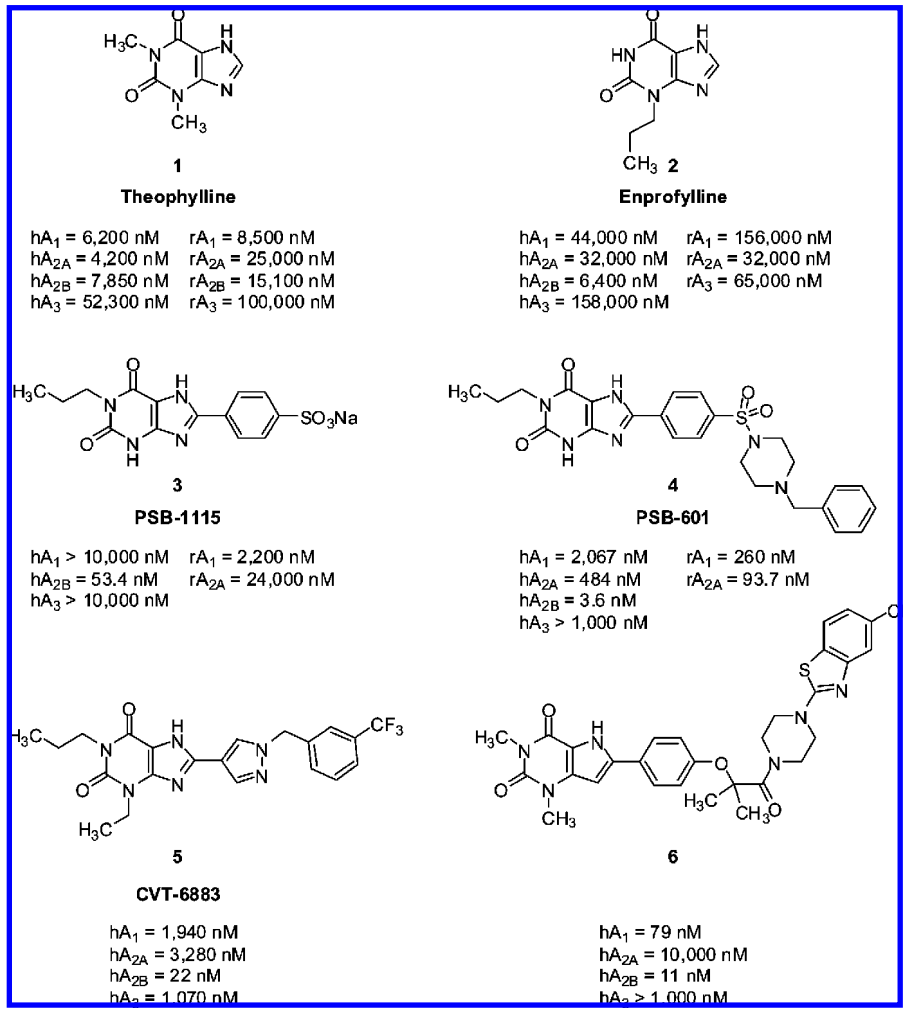

In vivo experiments showed that the A_{2B} antagonist CVT-6883 (**5**) reduced pulmonary inflammation and fibrosis in ADA-deficient mice as well as in mice with lung injury induced by bleomycin pretreatment.[25] It was also found that A_{2B} antagonist treatment reduced airway reactivity to NECA, AMP (which is converted to adenosine in vivo), or allergen challenge in an allergic mouse model of asthma.[26] Compound **5** is currently evaluated for cardiopulmonary disease in an ascending-dose phase I clinical study by CV Therapeutics, representing the first A_{2B} antagonist in clinical trials.[27] Thus, the asthmatic response to adenosine is likely to be mediated via A_{2B}AdoR, providing a firm basis for the development of A_{2B} antagonists as new antiasthmatic agents.[28]

The A_{2B}AdoR antagonists 8-(*p*-bromophenyl)-1-propargylxanthine (PSB-50), 4-(1-butylxanthin-8-yl)benzoic acid (PSB-53), 8-(4-(2-(4-benzylpiperazin-1-yl)-2-oxoethoxy)phenyl)-1-butylxanthine (PSB-55), and PSB-1115 (**3**) were tested among other subtype-selective AdoR antagonists for their analgesic potency in mice using the hot plate test. Unlike the tested A_1-, A_{2A}-, and A_3-selective antagonists, all four A_{2B}AdoR antagonists exhibited dose-dependent antinociceptive effects.[29] Moreover, **3** in combination with morphine showed a synergistic effect in the hot plate test and potently diminished inflammatory pain in mice during the second inflammatory phase after formalin injection.[29,30] These results suggest that selective A_{2B}AdoR antagonists could serve as drugs for the treatment of inflammatory pain, as a monotherapy or in combination with other analgesic drugs.

Adenosine was shown to stimulate IL-6 secretion to the luminal compartment in the human intestinal epithelial cell line T84 via cyclic AMP (cAMP) formation by activation of A_{2B}AdoR.[31,32] Upregulation of A_{2B}AdoR in mice with dextran sodium sulfate (DSS)-induced colitis and in intestinal epithelial mucosa of patients with colitis has been observed as well as TNF_α-induced upregulation of A_{2B}AdoR.[33] The potential proinflammatory role of the A_{2B}AdoR in colon was further investigated with A_{2B}AdoR knockout mice, which were found to develop an attenuated grade of colonic inflammation in comparison to the wild-type mice after treatment with DSS, 2,4,6-trinitrobenzene sulfonic acid (TNBS), or *Salmonella typhimurium*, respectively.[34] Moreover, it has been shown that the A_{2B}AdoR antagonist *N*-(5-(1-cyclopropyl-2,6-dioxo-3-propyl-2,3,6,7-tetrahydro-1*H*-purin-8-yl)pyridin-2-yl)-*N*-ethylnicotinamide (ATL-801) significantly suppressed proinflammatory cytokines and reduced the symptoms of colitis in DSS-treated and piroxicam-treated IL-$10^{-/-}$ mice, indicating that A_{2B}AdoR antagonists might serve as anti-inflammatory drugs for the treatment of colonic inflammation.[35,36]

Another potential field of application for A_{2B} antagonists might be the attenuation of neurodegenerative disorders such as Alzheimer's disease. A_{2B}AdoR have been shown to mediate IL-6 release in human astrocytoma cells[37] and to enhance astrogliosis in the presence of TNF_α in human astrocytoma cells,[38] both effects being important for the development of neurodegeneration.

Downloaded by UNIV OF NEWCASTLE on October 11, 2009 | http://pubs.acs.org
Publication Date (Web): May 27, 2009 | doi: 10.1021/jm900413e

Chart 2. Selective A_{2B} Antagonist Radioligands with K_D Values and Specific Activities for the A_{2B}AdoR and AdoR Affinities of Their Unlabeled Analogues[41,43,44,46,47,52−55]

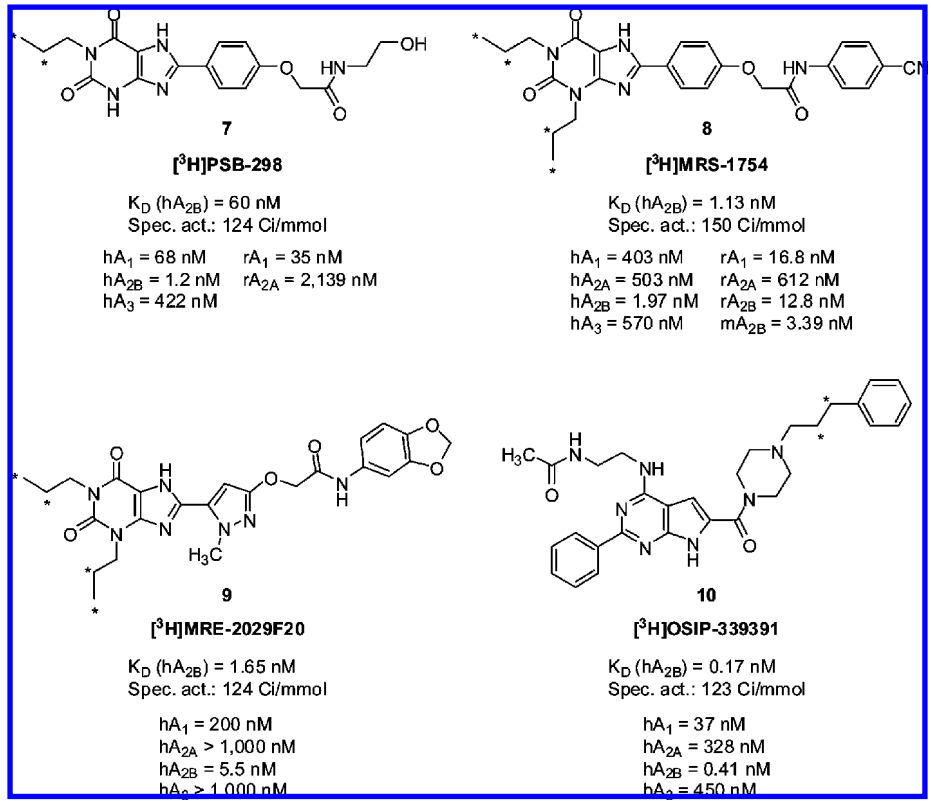

A recent study showed that A_{2B}AdoR knockout mice exhibit attenuated tumor growth and decreased levels of vascular endothelial growth factor (VEGF) in the tumors after inoculation with Lewis lung carcinoma when compared to wild-type mice, pointing at the involvement of A_{2B}AdoR activation in the neovascularization of tumors. The release of VEGF was increased by the nonselective agonist NECA but not by the A_{2A}-selective AdoR agonist 2-*p*-(2-carboxyethyl)phenethylamino-5′-*N*-ethylcarboxamidoadenosine (CGS-21680), whereas a combination of NECA and the selective A_{2B}AdoR antagonist **5** did not show this effect, indicating that A_{2B} antagonists might have the potential to inhibit tumor vascularization.[39]

In Chart 1, selected A_{2B} antagonists are shown. Theophylline (**1**) and enprofylline (**2**)[40] are currently used for the treatment of asthma. Their antiasthmatic effects have recently been attributed to the antagonism of the A_{2B}AdoR; however both compounds are weak A_{2B} antagonists and not or only moderately selective.[12] Intensified research led to the development of more selective high-affinity A_{2B} antagonists with a xanthine scaffold, namely **3**,[41] PSB-601 (**4**),[42] **5**,[27] PSB-298 (**7**),[41] **8**,[43] and MRE-2029F20 (**9**),[44] the deazaxanthine **6**,[45] and the deazaadenine derivative OSIP-339391 (**10**).[46] However, the majority of the nonxanthine A_{2B} antagonists developed so far is characterized by only moderate selectivity toward other AdoR subtypes. The xanthine-based A_{2B} antagonists currently show the most promising combination of high affinity and selectivity, but they often suffer from poor water solubility and thus low oral bioavailability.[47−49]

The A_{2B}AdoR has been cloned from rats, mice, and humans, showing high structural homologies between these species (87% human vs rat or mouse; 95% rat vs mouse).[50] Nevertheless, it has been reported that AdoR affinities of A_{2B} antagonists can vary between different species. Kim et al. found that the xanthine derivatives that they investigated bound with 2−9-fold lower affinities to the rat than to the human A_{2B}AdoR.[51] On the other hand, Kim et al.[43] as well as Yan et al.[42] observed that the xanthine derivatives tested in their studies were more potent at rat than at human A_1AdoR. This could mean that A_{2B} antagonists, which are very selective in humans may be less selective or even nonselective in rodents. For example, **8** is selective in humans but nonselective vs A_1 in rodents (see Chart 2).

High affinity, selectivity, and sufficient water solubility are pivotal properties for the development of new A_{2B} radioligands. The recently developed antagonist radioligands [^{3}H]**7**,[52] [^{3}H]**8**,[53] [^{3}H]**9**,[54] and [^{3}H]**10**[55] show K_D values in the low nanomolar range for the human A_{2B}AdoR. However, **7**, **9**, and **10** show selectivities of less than 100-fold vs human hA_1AdoR, and further improvement in selectivity is desirable. Compound **8** was recently tested for its affinity at A_{2B} receptors of different species, revealing a K_i value of 12.8 nM for the rA_{2B}AdoR, which means that the compound is nonselective in rat because it is similarly potent at rat A_1AdoR (K_i = 16.8 nM).[50] Its 205-fold selectivity in humans (A_{2B} vs A_1) further supports the hypothesis mentioned above that A_{2B} selectivity in rodents seems to be more difficult to achieve than in humans. To our knowledge, the recently developed high-affinity A_{2B} antagonists were exclusively tested at the human and not at rodent A_{2B} receptors. So far, only antagonist radioligands have been developed for the A_{2B}AdoR and the use of nonselective A_{2B} radioligands is still frequently reported.

On the basis of the most potent A_{2B} antagonists, a pharmacophore model has recently been developed by our group (Chart 3).[42] This model is characterized by a flat central core, which is a deazapurine or frequently a xanthine scaffold for most of the selective A_{2B} antagonists. The core is characterized by a hydrogen bond acceptor (e.g., C6-oxygen in xanthines) and a hydrogen bond donor (e.g., N7-hydrogen in xanthines). The lipophilic domains L1 and L2 allow for an introduction of alkyl

Downloaded by UNIV OF NEWCASTLE on October 11, 2009 | http://pubs.acs.org
Publication Date (Web): May 27, 2009 | doi: 10.1021/jm900413e

Chart 3. Pharmacophore Model for A_{2B} Antagonists and Structure of **4**[42]

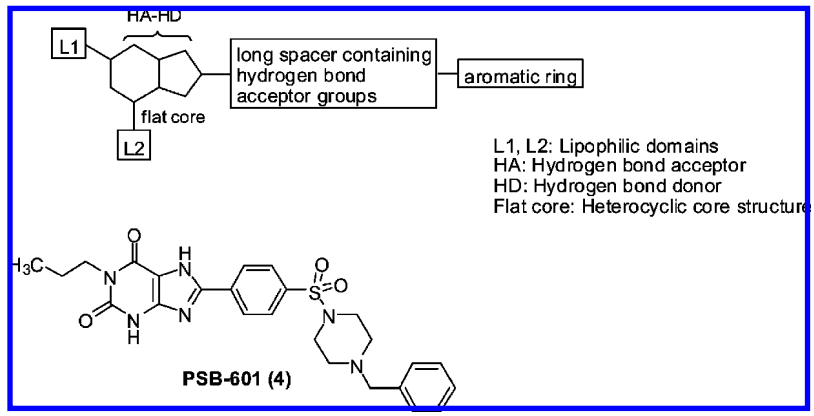

Scheme 1. Preparation of Sulfonamides **15**−**43**[a,b]

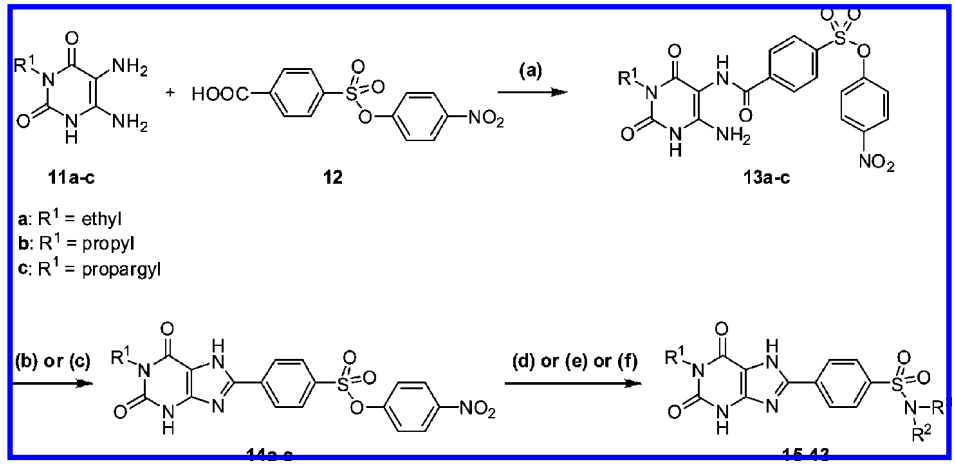

[a] Reagents and conditions: (a) EDC, MeOH, rt, 4 h. (b) For **14a** and **14b**: PPSE; (1) 120 °C, 10 min; (2) 170 °C, 2 h, MeOH. (c) For **14c**: HMDS, $(NH_4)_2SO_4$, reflux, 16 h, MeOH. (d) (1) DMF, rt, 2 d; (2) reflux, 1 h (method A). (e) (1) DMF, rt, 2 d; (2) reflux, 1 h; (3) aq NH_4OH (12.5%), 60 °C, 20 min (method B). (f) (1) DMF, rt, 2 d; (2) aq NH_4OH (12.5%), 60 °C, 20 min (method C). [b] For R^1, R^2, and R^3, see Table 1.

Downloaded by UNIV OF NEWCASTLE on October 11, 2009 | http://pubs.acs.org
Publication Date (Web): May 27, 2009 | doi: 10.1021/jm900413e

residues at positions 1 and 3. A small alkyl substituent (propyl, ethyl, methyl) at position 1 proved to increase A_{2B}AdoR affinity, whereas additional alkylation at position 3 led to a decrease in A_{2B}AdoR affinity and an increase in A_1 and A_{2A}AdoR affinity.[41] Position 8 is substituted with a spacer featuring hydrogen bond donor and acceptor groups, which is further connected to an aromatic residue. Taking **4** as a lead structure, we varied the substituent L1, the spacer, and the aromatic residue, whereas residue L2 was retained as a hydrogen atom, which was optimal for high affinity as well as selectivity.[41]

The aim of this study was to develop high-affinity A_{2B} antagonists exhibiting high selectivity in humans as well as rodents and to provide a new, improved A_{2B} antagonist radioligand on the basis of the obtained structure−activity relationships.

Results and Discussion

The target compounds were synthesized as depicted in Scheme 1. 3-Substituted 5,6-diaminouracils **11a**−**c**[56−58] and 4-(*p*-nitrophenoxysulfonyl)benzoic acid **12**[59] were obtained according to previously described procedures. Amide coupling of **11a**−**c** with **12** was performed with *N*-(3-(dimethylamino)-propyl)-*N*′-ethylcarbodiimide (EDC) as condensing agent to yield amides **13a**−**c**.[59] Ring closure of **13a**−**c** to the corresponding xanthine derivatives **14a**−**c** was achieved by heating with polyphosphoric acid trimethylsilyl ester (PPSE) in cases of 1-ethyl and 1-propyl substitution (**14a**, **14b**).[59] It had been reported that the use of PPSE in the case of 1-propargyl substitution leads to the formation of tricyclic oxazolo[3,2-*a*]-purinones.[60] Therefore, heating of **13c** with 1,1,1,3,3,3-hexamethyldisilazane (HMDS) in the presence of ammonium sulfate[61] was applied instead to afford compound **14c**. Sulfonamides **15**−**43** were obtained by aminolysis of *p*-nitrophenylsulfonates[42] and were subsequently purified by reverse-phase high performance liquid chromatography (RP-HPLC) (method A). However, in the cases of phenylpiperazinyl-substituted derivatives **34**−**38**, the sulfonamides could not be separated from unreacted starting compounds (esters **14a**−**c**) by chromatographic methods. Therefore, the product mixtures were subjected to alkaline hydrolysis in ammonia (pH 11; 60 °C; 20 min), resulting in hydrolysis of the esters **14a**−**c**, which were present as impurities. After evaporation of the ammonia and purification by RP-HPLC (methods B and C), the pure sulfonamides **34**−**38** were obtained. The synthesized xanthine-8-yl-benzenesulfonamides are collected in Table 1. The structures of all final products were confirmed by ^{1}H NMR and ^{13}C NMR spectroscopy and by mass spectrometry employing electron spray ionization (ESI). Purity was determined by elemental analysis and by RP-HPLC analysis coupled to UV detection at 254 nm and found to be ≥95% in all cases.

Biological Evaluation. The affinities of the xanthine-8-yl-benzenesulfonamide derivatives were determined in radioligand

Table 1. Methods, Isolated Yields, and Melting Points of Synthesized Xanthine-8-yl-benzenesulfonamide Derivatives

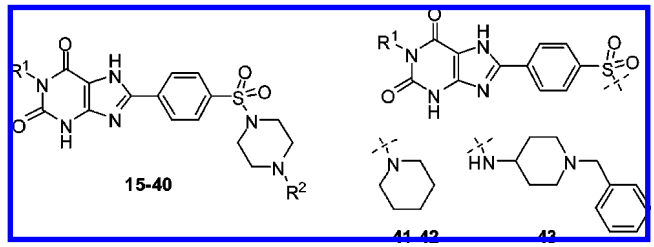

compd	R^1	R^2	precursor	method[a]	yield, %	melting point, °C (dec.)
			Benzylpiperazine Derivatives			
15	ethyl	benzyl	**14a**	A	77	>308
16	ethyl	4-chlorobenzyl	**14a**	A	63	>289
17 (PSB-0788)	propyl	4-chlorobenzyl	**14b**	A	64	>292
18	ethyl	3-chlorobenzyl	**14a**	A	66	>315
19	propyl	3-chlorobenzyl	**14b**	A	62	>293
20	ethyl	4-fluorobenzyl	**14a**	A	46	>289
21	propyl	4-fluorobenzyl	**14b**	A	49	>286
22	ethyl	3-fluorobenzyl	**14a**	A	63	>310
23	propyl	3-fluorobenzyl	**14b**	A	80	>295
24 (PSB-09120)	ethyl	4-(trifluoromethyl)benzyl	**14a**	A	50	>310
25	propyl	4-(trifluoromethyl)benzyl	**14b**	A	68	>290
26	ethyl	3-(trifluoromethyl)benzyl	**14a**	A	56	>288
27	propyl	3-(trifluoromethyl)benzyl	**14b**	A	65	>294
28	ethyl	4-methylbenzyl	**14a**	A	38	>283
29	propyl	4-methylbenzyl	**14bv**	A	75	>283
30	ethyl	4-methoxybenzyl	**14a**	A	61	>278
31	propyl	4-methoxybenzyl	**14b**	A	69	>278
32	ethyl	3,4-(methylenedioxy)benzyl	**14a**	A	57	>288
33	propyl	3,4-(methylenedioxy)benzyl	**14b**	A	59	>276
			Phenylpiperazine Derivatives			
34	ethyl	4-chlorophenyl	**14a**	B	49	>308
35 (PSB-603)	propyl	4-chlorophenyl	**14b**	B	62	>298
36	propargyl	4-chlorophenyl	**14c**	C	38	>274
37	ethyl	4-methoxyphenyl	**14a**	B	39	>265
38	propyl	4-methoxyphenyl	**14b**	B	47	>270
			Phenethylpiperazine Derivatives			
39	ethyl	phenethyl	**14a**	A	71	>280
40	propyl	phenethyl	**14b**	A	69	>288
			Piperidine Derivatives			
41	ethyl	see structure above	**14a**	A	71	>343
42	propyl	see structure above	**14b**	A	78	>332
			Benzylpiperidinylamine Derivative			
43	propyl	see structure above	**14b**	A	38	>271

[a] For methods A, B, and C, see general procedures in Experimental Section.

Downloaded by UNIV OF NEWCASTLE on October 11, 2009 | http://pubs.acs.org
Publication Date (Web): May 27, 2009 | doi: 10.1021/jm900413e

binding studies at A_1, A_{2A}, A_{2B}, and A_3AdoR using [^{3}H]2-chloro-N^6-cyclopentyladenosine ([^{3}H]CCPA), [^{3}H](*E*)-3-(3-hydroxypropyl)-8-(2-(3-methoxyphenyl)vinyl)-7-methyl-1-prop-2-ynyl-3,7-dihydropurine-2,6-dione ([^{3}H]MSX-2), [^{3}H]8-(4-(4-(4-chlorophenyl)piperazine-1-sulfonyl)phenyl)-1-propyl-3,7-dihydropurine-2,6-dione ([^{3}H]**35**), and [^{3}H]2-phenyl-8-ethyl-4-methyl-(8*R*)-4,5,7,8-tetrahydro-1*H*-imidazo[2.1-*i*]purin-5-one ([^{3}H]PSB-11) as A_1, A_{2A}, A_{2B}, and A_3 radioligands, respectively.[62−65] Rat brain cortical membranes were used as a source for the rat A_1AdoR, rat brain striatal membranes for rat A_{2A}AdoR. Assays at the A_{2B} and A_3AdoR were performed with human receptors recombinantly expressed in Chinese hamster ovary (CHO) cells.[66] Selected compounds were additionally tested at the human A_1 and A_{2A}AdoR, and the mouse A_{2B}AdoR recombinantly expressed in CHO cells.[66] Functional calcium assays of selected compounds were performed at Jurkat T cells, a human lymphoma cell line.[67]

Structure−Activity Relationships. The first 13 compounds synthesized in this series were tested in a functional assay at the human A_{2B}AdoR by measuring the inhibition of the NECA-induced A_{2B}-mediated increase in the intracellular calcium concentration ($[Ca^{2+}]_i$) in Jurkat T cells.[67] A_{2B} receptors were stimulated by NECA (10 μM),[67] resulting in an increase in calcium concentration (Figure 1). This effect appeared to be due to A_{2B} as well as A_{2A}AdoR activation. The A_{2A} component was blocked by a high concentration of the A_{2A}-selective antagonist MSX-2[68] (200 nM) (Figure 1). Therefore, the functional experiments were performed in the presence of 200 nM MSX-2 to exclude potential A_{2A}-mediated effects of the tested compounds.[68]

Selectivities over the other AdoR were determined by radioligand binding studies at the rat A_1 and A_{2A}AdoR and at the human recombinant A_1, A_{2A}, and A_3AdoR. The best compound was further tested at recombinant mouse A_{2B} receptors in order to investigate potential species differences. After development of the new potent and selective A_{2B} radioligand **35**, all compounds were investigated in radioligand binding assays versus [^{3}H]**35** at human A_{2B} receptors

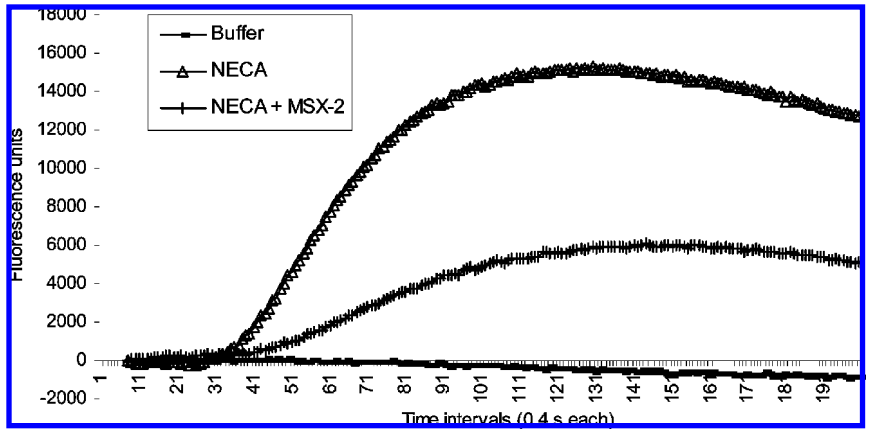

Figure 1. NECA (10 μM) induced calcium signal in the presence and in the absence of the A_{2A}AdoR antagonist MSX-2 (200 nM). A representative curve out of three independent experiments is shown.

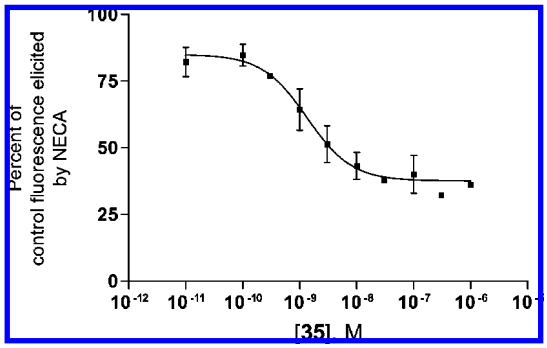

Figure 2. Concentration-dependent inhibition of A_{2B}-mediated calcium response in Jurkat T cells by **35**. Cells were stimulated with 10 μM NECA in the presence of 200 nM MSX-2 to block A_{2A} receptors. Oregon Green was used as a fluorescent indicator of the intracellular calcium concentration. Data points are means ± SEM of three experiments.

Downloaded by UNIV OF NEWCASTLE on October 11, 2009 | http://pubs.acs.org
Publication Date (Web): May 27, 2009 | doi: 10.1021/jm900413e

expressed in CHO cells. All tested compounds showed high potency at the A_{2B}AdoR with IC_{50} values in the nanomolar range (Table 2).

All of the initial series of compounds tested were potent A_{2B} antagonists at Jurkat T cells exhibiting IC_{50} values between 1.13 nM (**35**) and 16.2 nM (**31**). Propyl and ethyl substitution at N1 were similarly well tolerated (compare **26** and **27**). The terminal benzyl residues at the piperazine ring could be substituted in the meta- or para-position (compare **17**/**19** and **25**/**27**) without much change in potency. However, 3,4-methylenedioxybenzyl substituents were somewhat less well tolerated (**33**) when combined with a 1-propyl residue. Phenethyl substitution as in compound **40** was also slightly disadvantageous when compared to the benzyl derivatives. The most potent and selective A_{2B} antagonist in this series was compound **35**, exhibiting an IC_{50} value of 1.13 nM and virtually no affinity for all other AdoR subtypes up to a concentration of 10 μM. The concentration−inhibition curve for compound **35** at the human A_{2B} receptor in Jurkat T cells is shown in Figure 2.

Thus, we selected this A_{2B}-specific antagonist for radiolabeling in order to obtain an A_{2B} radioligand for further studying the structure−activity relationships of this class of compounds. This was achieved by catalytic hydrogenation of the 1-propargyl-substituted precursor **36** with tritium gas in the presence of Pd/C (10%) in ethanol/dimethylformamide (DMF) affording the new radioligand [^{3}H]**35** after purification with RP-HPLC (Scheme 2). The labeling reaction was performed by GE Healthcare UK Limited. The identity of [^{3}H]**35** was confirmed by mass spectrometric analysis, and [^{3}H]**35** displayed a specific activity of 2.70 TBq/mmol (73 Ci/mmol) and a radiochemical purity of 98.9% as determined by HPLC/UV (254 nm).

[^{3}H]**35** was found to bind with high affinity to human A_{2B}AdoR stably expressed in CHO cells. Membrane preparations thereof containing 30 μg protein/vial were used to characterize the new radioligand in kinetic, saturation, and competition binding experiments. Kinetic as well as competition experiments were performed with a radioligand concentration of 0.3 nM in the presence of 2 U/mL adenosine deaminase with a dimethylsulfoxide (DMSO) concentration not exceeding 2.5% in 50 mM Tris buffer pH 7.4. The specific binding amounted to ca. 70% of total binding. Thus, the nonspecific binding of [^{3}H]**35** was comparable to the degree of nonspecific binding reported for other selective A_{2B} antagonist radioligands.[52,53,55,69] A direct comparison with literature data is not possible because the relationship of specific to nonspecific binding is highly dependent on the receptor expression level. Incubation was terminated by rapid filtration through GF/B glass-fiber filters and subsequent washing with 4 × 3 mL of ice-cold Tris-buffer containing 0.1% bovine serum albumin (BSA). For kinetic studies, 30 μg of protein was incubated with the radioligand for 180 min (association kinetics). Dissociation was initiated by addition of 10 μM 8-cyclopentyl-1,3-dipropylxanthine (DPCPX) after 95 min of preincubation. Equilibrium binding was reached after less than 60 min and was stable for at least 3 h at room temperature (Figure 3A). Radioligand binding was reversible after addition of DPCPX. A kinetic K_D value of 0.652 ± 0.269 nM was calculated from the association and dissociation constants (Figure 3).

The saturation experiments were performed with 30 μg of protein (CHO cell membranes expressing the human A_{2B}AdoR) and [^{3}H]**35** in a concentration range of 0.05 nM to 1 nM. A K_D value of 0.403 ± 0.188 nM was obtained and a B_{max} value of 502 ± 57 fmol/mg protein was calculated. This K_D value was in close agreement with the K_D value obtained from the kinetic experiments (Figure 4).

Competition binding experiments with standard AdoR agonists and antagonists were performed using a radioligand concentration of 0.3 nM, an incubation time of 75 min in 50 mM Tris buffer pH 7.4, and a protein amount of 30 μg per tube (Figure 5). The K_i values determined with the new radioligand binding assay were in accordance with previously published data (Table 3). The rank order of potency was consistent with specific labeling of an A_{2B}AdoR, demonstrating

Table 2. AdoR Affinities of Xanthine-8-yl-benzenesulfonamide Derivatives

	$K_i \pm$ SEM [nM] (or % inhibition of radioligand binding at indicated concentration ± SEM)						$IC_{50} \pm$ SEM [nM]
	A_1 rat brain cortical membranes[a]	A_1 human recombinant[a]	A_{2A} rat brain striatal membranes[b]	A_{2A} human recombinant[b]	A_{2B} human recombinant[c]	A_3 human recombinant[d]	A_{2B} Jurkat T cells (human)[e]
				Benzylpiperazine Derivatives			
4	260 ± 0[42]	2067 ± 261[42]	93.7 ± 32.1[42]	484 ± 115[42]	3.6 ± 0.4[42f]	>1000[42] (29)[g]	10.1 ± 1.6
15	250 ± 49	1840 ± 530	335 ± 52	152 ± 66	1.15 ± 0.07	>10000 (27 ± 10)[h]	4.49 ± 2.88
16	2730 ± 1430	>10000 (18 ± 9)[h]	445 ± 141	6.49 ± 2.19	0.215 ± 0.067	>10000 (10 ± 18)[h]	nd
17	386 ± 98	2240 ± 959	1730 ± 790	333 ± 84	0.393 ± 0.085	>1000 (18 ± 1)[g]	3.64 ± 0.98
18	96.7 ± 7.8	nd	263 ± 93	nd	0.610 ± 0.239	557 ± 217	nd
19	178 ± 38	1090 ± 250	799 ± 358	161 ± 42	0.782 ± 0.195	24200 ± 9700	1.91 ± 0.08
20	296 ± 43	1820 ± 660	40.2 ± 14.2	92.0 ± 41.3	1.27 ± 0.60	>1000 (21 ± 2)[g]	nd
21	33.8 ± 2.0	nd	194 ± 55	nd	0.595 ± 0.101	758 ± 229	nd
22	359 ± 86	2070 ± 1120	388 ± 149	144 ± 62	0.695 ± 0.199	5780 ± 960	nd
23	111 ± 43	2300 ± 430	782 ± 236	278 ± 121	0.446 ± 0.129	>1000 (32 ± 7)[g]	3.23 ± 0.19
24	>1000 (14 ± 2)[g]	>10000 (25 ± 3)[h]	122 ± 36	22.7 ± 8.5	0.157 ± 0.062	>10000 (13 ± 5)[h]	nd
25	463 ± 122	5630 ± 490	1540 ± 271	145 ± 14	0.303 ± 0.153	>10000 (44 ± 7)[h]	1.62 ± 0.69
26	564 ± 180	2300 ± 410	635 ± 212	69.4 ± 57.2	0.281 ± 0.016	>10000 (38 ± 4)[h]	2.29 ± 0.58
27	273 ± 47	2610 ± 222	1700 ± 217	306 ± 140	0.775 ± 0.214	30000 ± 22000	3.56 ± 0.20
28	39.0 ± 9.0	nd	341 ± 76	nd	1.58 ± 0.35	>1000 (22 ± 10)[g]	nd
29	46.7 ± 12.4	nd	1750 ± 480	nd	0.858 ± 0.151	156 ± 35	nd
30	354 ± 134	3800 ± 820	914 ± 343	236 ± 40	1.19 ± 0.37	>1000 (29 ± 15)[g]	5.26 ± 1.00
31	83.8 ± 18.9	>10000 (38 ± 6)[h]	1020 ± 561	328 ± 59	0.944 ± 0268	>10000 (23 ± 10)[h]	16.2 ± 6.3
32	272 ± 108	>10000 (28 ± 9)[h]	436 ± 48	102 ± 33[i]	0.875 ± 0.224	>10000 (32 ± 7)[h]	5.34 ± 2.06
33	79.4 ± 4.7	443 ± 113	590 ± 29	112 ± 3	1.06 ± 0.37	17600 ± 1400	23.4 ± 10.3
				Phenylpiperazine Derivatives			
34	>10000 (48 ± 3)[h]	>1000 (−7 ± 4)[g]	119 ± 83	48.4 ± 10.9	0.406 ± 0.142	434 ± 143	nd
35	>10000 (18 ± 1)[h]	>10000 (10 ± 3)[h]	>10000 (19 ± 5)[h]	>10000 (7 ± 14)[h]	0.553 ± 0.103	>10000 (10 ± 15)[h]	1.13 ± 0.39
36	1440 ± 50	nd	198 ± 88	nd	0.473 ± 0.067	>1000 (35 ± 2)[g]	nd
37	>1000 (30 ± 6)[g]	nd	367 ± 44	nd	11.7 ± 1.8	>1000 (−19 ± 20)[g]	nd
38	>1000 (27 ± 4)[g]	>10000(−17 ± 14)[h]	41.5 ± 15.3	3720 ± 1060	1.99 ± 0.37	>1000 (1 ± 7)[g]	nd
				Phenethylpiperazine Derivatives			
39	86.8 ± 46.1	nd	ca. 1000(56 ± 7)[g]	nd	7.49 ± 1.20	>1000 (−17 ± 12)[g]	nd
40	>10000 (42 ± 8)[h]	>10000 (39 ± 4)[h]	681 ± 337	271 ± 127[i]	7.51 ± 1.84	>1000 (30 ± 16)[g]	10.9 ± 3.3
				Piperidine Derivatives			
41	77.1 ± 22.9	nd	251 ± 87	nd	5.43 ± 0.61	209 ± 57	nd
42	91.1 ± 25.0	nd	714 ± 122	nd	19.7 ± 4.7	140 ± 20	nd
				Benzylpiperidinylamine Derivative			
43	38.5 ± 4.5	1170 ± 64	136 ± 16	94.5 ± 30.8	3.03 ± 0.55	2080 ± 410	nd

[a] Versus [^{3}H]CCPA ($n = 3$). [b] Versus [^{3}H]MSX-2 ($n = 3$, unless otherwise noted). [c] Versus [^{3}H]**35** ($n = 3$). [d] Versus [^{3}H]PSB-11 ($n = 3$). [e] Calcium assay ($n = 3$). [f] Versus [^{3}H]**7**.[42] [g] Inhibition of radioligand binding at 1 μM ± SEM. [h] Inhibition of radioligand binding at 10 μM ± SEM. [i] $n = 4$.

Scheme 2. Preparation of the New A_{2B}-Specific Radioligand [^{3}H]**35** by Catalytic Hydrogenation of its Propargyl Precursor

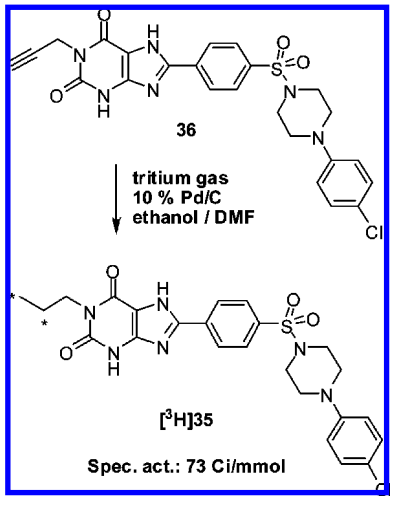

that [^{3}H]**35** will be a useful tool for the identification of new A_{2B}AdoR ligands.

To investigate whether the new radioligand was also suitable for the labeling of rodent A_{2B}AdoR, we performed a homologous competition experiment at CHO cells that stably express the mouse A_{2B} receptor (see Figure 6). Applying the same conditions as for the human A_{2B} receptors, we observed a similarly high affinity for the mouse A_{2B} receptor as well. The calculated K_D value was 0.351 nM at the mouse A_{2B}AdoR and thus almost identical to that determined at the human receptor (0.403 nM). These results show that [^{3}H]**35** can be used for the labeling of human as well as rodent A_{2B} receptors; it does not only show high affinity but also very high selectivity in humans as well as rodents (see Table 2).

All synthesized compounds of the xanthine-8-yl-benzenesulfonamide series were then tested in competition binding experiments at human A_{2B}AdoR versus the new radioligand [^{3}H]**35**. The obtained K_i values correlated quite well with the IC_{50} values obtained in the functional calcium assays at Jurkat T cells, confirming the suitability of the newly established assays (Table 2). The A_{2B} K_i values of 12 compounds of the present series were in the nanomolar range, and 17 compounds exhibited affinities even in the subnanomolar range. This fact demonstrated clearly that the synthesized xanthine-8-yl-benzenesulfonamides represent a class of very potent A_{2B} antagonists. As expected, most of the tested compounds showed virtually no affinity for the human A_3AdoR and a good selectivity versus A_1 and A_{2A}AdoR, confirming the previously reported finding that 1-monosubstitution leads to higher A_{2B} affinity and enhanced selectivity when compared to 1,3-disubstitution.[41,42,59] Interest-

Downloaded by UNIV OF NEWCASTLE on October 11, 2009 | http://pubs.acs.org
Publication Date (Web): May 27, 2009 | doi: 10.1021/jm900413e

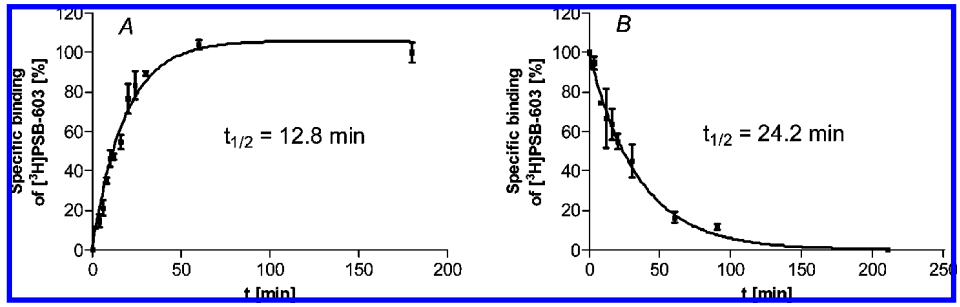

Figure 3. Kinetics of [^{3}H]**35** binding to the human A_{2B}AdoR recombinantly expressed in CHO cells. (A) Association curve, (B) dissociation curve. Dissociation was initiated by the addition of 10 μM DPCPX after 95 min of preincubation. Data points are means of two experiments performed in duplicates.

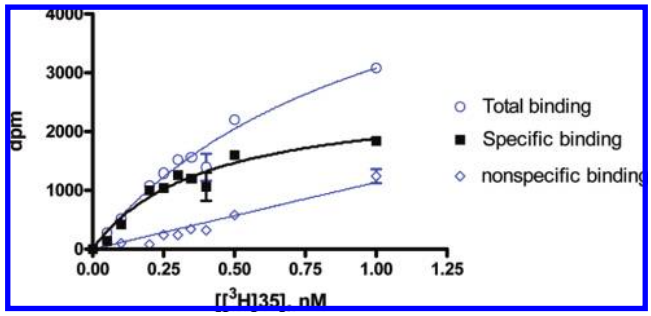

Figure 4. Saturation binding of [^{3}H]**35** to the human A_{2B}AdoR recombinantly expressed in CHO cells. Data points represent means from a typical experiment performed in duplicates.

Downloaded by UNIV OF NEWCASTLE on October 11, 2009 | http://pubs.acs.org
Publication Date (Web): May 27, 2009 | doi: 10.1021/jm900413e

ingly, the tested A_{2B} antagonists were about 10-fold more potent at the rat A_1AdoR than at the human A_1AdoR, whereas the K_i values at the rat A_{2A}AdoR were in most cases 3−10-fold higher than those determined at the human A_{2A}AdoR. This observation is illustrated by a correlation of the pK_i values of the synthesized A_{2B} antagonists for the rat and the human A_1 and A_{2A}AdoR subtypes (Figure 7). For the A_1AdoR, all data points are above the line meaning higher affinity for the rat than for the human A_1AdoR, whereas for the A_{2A}AdoR, the correlation is much better. These findings are in accordance with previously observed species differences,[42,43,51] suggesting that the dependency of AdoR affinities on the species represents an important issue that should be addressed in further studies evaluating AdoR ligand affinities and selectivities.[50]

As already observed in the initial functional experiments, 1-ethyl- and 1-propyl-substituted xanthines showed very similar affinities for the A_{2B}AdoR (compare **16**/**17**, **18**/**19**, **24**/**25**, **30**/**31**, **39**/**40**). Likewise, 1-propargyl substitution in case of compound **36** resulted in an A_{2B}AdoR affinity (K_i = 0.473 nM), which was very similar to those of the corresponding ethyl (**34**, K_i = 0.406 nM) and propyl (**35**, K_i = 0.553 nM) analogues. On the other hand, most 1-ethyl derivatives showed higher affinity than the corresponding 1-propyl derivatives for the rat A_{2A} receptor, indicating that 1-propyl substitution was favorable in terms of improved A_{2B}/A_{2A} selectivity.

The variation of the spacer and the aromatic residue at position 8 of the xanthine core led to the main finding that benzylpiperazinyl and phenylpiperazinyl substitution appeared to be the best tolerated modification for the A_{2B}AdoR. Piperidine analogues **41** and **42** exhibited lower affinities than nearly all of the corresponding piperazine derivatives (K_i values of 5.43 nM and 19.7 nM, respectively). Also, phenethylpiperazine and benzylpiperidinylamino substituents (**39**, **40**, and **43**) were less tolerated by the A_{2B}AdoR (about 1 order of magnitude decrease in affinity) when compared to the corresponding benzylpiperazinyl- or phenylpiperazinyl-substituted derivatives, which mostly exhibited K_i values in the subnanomolar range. The most potent A_{2B} antagonist in this series was the 4-trifluoromethylbenzylpiperazine derivative **24** with a K_i value of 0.157 nM showing no detectable affinity for the A_1 and A_3AdoR. However, as many benzylpiperazine and phenylpiperazine derivatives, it exhibited some affinity for the A_{2A} receptor (K_i = 22.7 nM). Nevertheless, **24** was still >100-fold selective. Compound **17** showed the best profile of affinity and selectivity in the benzylpiperazine series (K_i = 0.393 nM; 5700-fold (vs hA_1), 870-fold (vs hA_{2A}), >2544-fold (vs hA_3)). The most selective A_{2B} antagonist was the corresponding 4-chlorophenyl-piperazinyl derivative **35** exhibiting a K_i value of 0.553 nM for the A_{2B}AdoR and no detectable affinity for the A_1, A_{2A}, and A_3AdoR, respectively, and therefore being, to our knowledge, the first A_{2B}-specific high-affinity antagonist. Because **35** is the corresponding cold ligand of the new radioligand described in this study, it can be stated that [^{3}H]**35** is the first A_{2B}-specific high-affinity radioligand.

As mentioned above, a major problem of many xanthine-based A_{2B} antagonists is their low water solubility and thus limited peroral bioavailability. To improve these properties, we had introduced basic nitrogen atoms as a part of the spacer in the substituted piperazine and 4-aminopiperidine derivatives offering the potential to form salts with increased solubility and bioavailability. To assess the physicochemical properties of this new series of A_{2B} antagonists, we calculated their pK_A values, polar surface areas (PSA), and log *P* values, which are important predictive parameters, employing the software MarvinSketch (pK_A and log *P* values) and Molinspiration (PSA values). The obtained results are listed in Table 4.

The benzyl- and phenethyl-piperazine derivatives **15**−**33**, and **39**−**40** showed calculated pK_A values in the range of 6.96−7.50, indicating that these compounds will be partly protonated under physiological conditions, which increases water solubility. Compounds **34**−**38** exhibited pK_A values in the range of 1−3 and will therefore be not protonated under physiological conditions, unless perhaps in the acidic medium of the stomach. Most of the compounds showed polar surface area (PSA) values of <140 Å^2, indicating that they may be intestinally absorbable.[71] The calculated log *P* values of all compounds were lower than 5, which is, according to Lipinski's rules,[72] the upper limit for drugs exhibiting suitable pharmacokinetic properties.

Conclusions

A series of xanthine-8-yl-benzenesulfonamide derivatives was synthesized as new selective high-affinity A_{2B} antagonists, tested in radioligand binding studies, and functionally characterized. On the basis of the obtained structure−activity relationships,

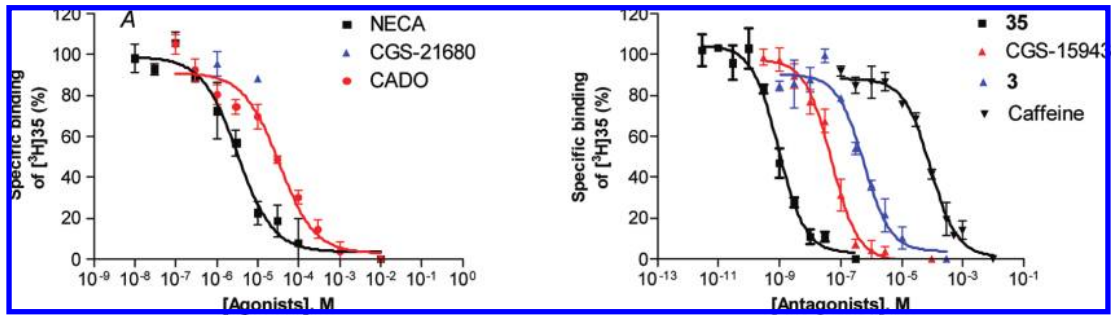

Figure 5. Inhibition of 0.3 nM [^{3}H]**35** binding to the human A_{2B}AdoR recombinantly expressed in CHO cells, (A) by the agonists NECA, CGS-21680, and 2-chloroadenosine (CADO), and (B) by the antagonists 9-chloro-2-(2-furanyl)-1,2,4-triazolo[1.5-*c*]quinazolin-5-amine (CGS-15943), **3**, caffeine, and unlabeled **35** (homologous competition). Data points are means ± SEM of three experiments performed in duplicates.

Table 3. A_{2B}AdoR Affinities of Selected Standard Agonists and Antagonists

	K_i ± SEM [μM] (or % inhibition of radioligand binding at indicated concentration)	
	human A_{2B}AdoR vs [^{3}H]**35**	human A_{2B}AdoR vs other radioligands
	Agonists	
NECA	1.89 ± 0.24	0.570 ± 0.170[53,a] 0.262 ± 0.030,[69,b]
CADO	21.4 ± 5.7	25.5 ± 6.2[40,c]
CGS-21680	(12 ± 1% at 10 μM)	(<10% at 100 μM)[70,d]
	Antagonists	
CGS-15943	0.0300 ± 0.0039	0.0342 ± 0.0010[53,a] 0.0164 ± 0.0036[70,d] 0.0098 ± 0.0009[69,b]
3	0.237 ± 0.050	0.0534 ± 0.0182[41,d]
caffeine	33.8 ± 1.2	10.4 ± 1.8[51,c]
4	0.00133 ± 0.00050	0.0036 ± 0.0004[42,e]

[a] Versus [^{3}H]**8**. [b] Versus [^{3}H]**9**. [c] Versus [^{125}I]I-ABOPX. [d] Versus [^{3}H]ZM-241385. [e] Versus [^{3}H]**7**.

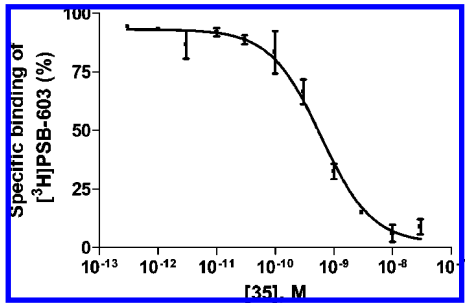

Figure 6. Homologous competition experiment: concentration-dependent inhibition of radioligand binding (0.3 nM [^{3}H]**35**) by compound **35** (unlabeled **35**) at membrane preparations of CHO cells recombinantly expressing the mouse A_{2B} receptor. The calculated K_D value was 0.351 ± 0.126 nM (n = 3). A B_{max} value of 645 ± 51 fmol/mg protein was determined.

the new A_{2B}-specific antagonist radioligand [^{3}H]**35** was developed and utilized in radioligand binding assays. In this study we developed, to our knowledge, the most potent A_{2B} antagonists known to date, **24** (K_i = 0.157 nM, 150-fold selective vs hA_{2A}, >60000-fold selective vs hA_1 and hA_3) and **17** (K_i = 0.393 nM, 850-fold selective vs hA_{2A}, >2500-fold selective vs hA_1 and hA_3). Both compounds feature a basic nitrogen atom that will increase water solubility and may improve bioavailability. The unlabeled analogue of the radioligand [^{3}H]**35** (K_i = 0.553 nM) represents, to our knowledge, the first high-affinity A_{2B}-specific antagonist for humans and rodents exhibiting no measurable affinity to any other AdoR subtype.

Experimental Section

All reagents were obtained from various producers (Acros, Aldrich, Fluka, Merck, and Sigma) and used without further purification. Solvents were used without additional purification or drying unless otherwise noted. Reactions were monitored by thin-layer chromatography (TLC) using aluminum sheets coated with silica gel 60 F_{254} (Merck). Compounds were visualized under UV light (254 nm). Preparative HPLC was performed on a Knauer HPLC system using a Wellchrome K-1800 pump, a WellChrome K-2600 spectrophotometer, and a Eurospher 100 C18 column (250 mm × 20 mm, particle size 10 μm). A gradient of methanol in water was used as indicated below with a flow rate of 20 mL/min. The purity of all tested compounds was determined by elemental analysis and by HPLC-UV obtained on an LC-MS instrument (Applied Biosystems API 2000 LC-MS/MS, HPLC Agilent 1100) using the following procedure: Compounds were dissolved at a concentration of 0.5 mg/mL in methanol. Then, 10 μL of the sample were injected into a Phenomenex Luna C18 HPLC column (50 mm × 2.00 mm, particle size 3 μm) and were chromatographed using a gradient of water: methanol (containing 2 mM ammonium acetate) from 90:10 to 0:100 for 30 min at a flow rate of 250 μL/min, starting the gradient after 10 min. UV absorption was detected from 200 to 950 nm using a diode array detector. Purity of the compounds was determined at 254 nm and proved to be ≥95%. Elemental microanalyses (C, H, N) were performed on a VarioEL apparatus and determined values are generally within ±0.4% of calculated values. Mass spectra were recorded on an API 2000 mass spectrometer (electron spray ion source, Applied Biosystems, Darmstadt, Germany) coupled with an Agilent 1100 HPLC system. ^{1}H and ^{13}C NMR spectra were recorded on a Bruker Avance 500 MHz NMR spectrometer. DMSO-d_6 was used as solvent. NMR spectra were recorded at rt. Shifts are given in parts per million (ppm) relative to the remaining protons of the deuterated solvent used as internal standard. Coupling constants J are given in Hertz, and spin multiplicities are given as s (singlet), d (doublet), t (triplet), q (quartet), m (multiplet), br (broad). Melting points were determined on a Büchi B-545 melting point apparatus and were uncorrected. Lyophilization was performed with a CHRIST ALPHA 1−4 LSC freeze-dryer.

General Procedure for the Amide Coupling of 11a−c with 12. 5,6-Diaminouracil **11a−c** (8.30 mmol) was dissolved in 40 mL methanol. 4-(4-Nitrophenoxysulfonyl)benzoic acid **12** (8.30 mmol) and EDC (9.10 mmol) were added, and the mixture was stirred for

Downloaded by UNIV OF NEWCASTLE on October 11, 2009 | http://pubs.acs.org
Publication Date (Web): May 27, 2009 | doi: 10.1021/jm900413e

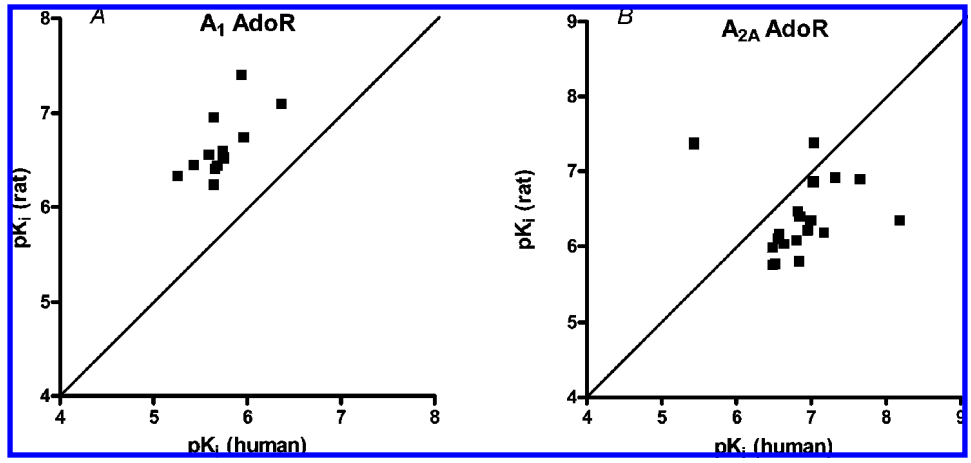

Figure 7. Comparison of the pK_i values of synthesized A_{2B} antagonists for the human and rat AdoR ((A) A_1AdoR; (B) A_{2A}AdoR).

Table 4. Calculated Physicochemical Properties of New A_{2B} Antagonists

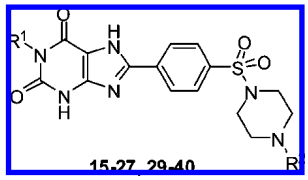

compd	R^1	R^2	calcd pK_A[a]	calcd PSA[b]	calcd log P[a]
		Benzylpiperazine Derivatives			
15	ethyl	1-benzyl	7.26	124.168	2.84
16	ethyl	4-chlorobenzyl	7.11	127.09	3.36
17	propyl	4-chlorobenzyl	7.11	124.168	3.83
18	ethyl	3-chlorobenzyl	7.07	127.09	3.36
19	propyl	3-chlorobenzyl	7.07	124.168	3.83
20	ethyl	4-fluorobenzyl	7.04	127.09	2.98
21	propyl	4-fluorobenzyl	7.04	127.09	3.45
22	ethyl	3-fluorobenzyl	6.96	127.09	2.98
23	propyl	3-fluorobenzyl	6.96	124.168	3.45
24	ethyl	4-(trifluoromethyl)benzyl	7.11	127.09	3.72
25	propyl	4-(trifluoromethyl)benzyl	7.11	124.168	4.19
26	ethyl	3-(trifluoromethyl)benzyl	7.07	124.168	3.72
27	propyl	3-(trifluoromethyl)benzyl	7.07	124.168	4.19
29	propyl	4-methylbenzyl	7.11	127.09	4.19
30	ethyl	4-methoxybenzyl	7.16	133.402	2.59
31	propyl	4-methoxybenzyl	7.16	133.402	3.06
32	ethyl	3,4-(methylenedioxy)benzyl	6.96	142.436	2.52
33	propyl	3,4-(methylenedioxy)benzyl	6.96	142.436	2.99
		Phenylpiperazine Derivatives			
34	ethyl	4-chlorophenyl	1.80	127.09	3.74
35	propyl	4-chlorophenyl	1.80	124.168	4.20
36	propargyl	4-chlorophenyl	1.78	127.09	3.83
37	ethyl	4-methoxyphenyl	3.02	133.402	2.97
38	propyl	4-methoxyphenyl	3.02	133.402	3.43
		Phenethylpiperazine Derivatives			
39	ethyl	phenethyl	7.50	127.09	3.09
40	propyl	phenethyl	7.50	124.168	3.56

[a] log P values and pK_A values for the benzyl-, phenyl-, or phenethyl-substituted nitrogen atom were calculated with the software MarvinSketch. [b] PSA values were calculated using the software Molinspiration.

5 h at rt. The formed precipitate was filtered off and washed with water. A sample was recrystallized from ethanol for analytical characterization. Yields ranged from 65% to 77%.

General Procedures for the Cyclization of the Xanthine Heterocycles. Compounds 14a−b. A mixture of carboxamido derivative **13a−b** (2.00 mmol) and 3.0 g of PPSE was heated for 10 min at 120 °C and then for 2 h at 170 °C. After cooling to rt, 20 mL of methanol were added and the resulting suspension was filtered and washed with methanol. Yields ranged from 80% to 86%.

Compound 14c. A mixture of carboxamido derivative **13c** (0.50 mmol), 0.1 g $(NH_4)_2SO_4$, and 10 mL HMDS was heated under reflux for 16 h. After cooling to rt, 20 mL of methanol were added and the resulting suspension was filtered off and washed with methanol, yielding the product in 70% yield.

General Procedures for the Aminolysis of *p*-Nitrophenylsulfonates. Method A. *p*-Nitrophenylsulfonate **14a−c** (0.22 mmol) was dissolved in 5 mL DMF, and the appropriate amine was added (2.2 mmol). The solution was stirred for 48 h at rt and subsequently refluxed for 1 h. The solvent was removed under reduced pressure, and the residue was dissolved in dichloromethane:methanol (20:1). Diethyl ether was added to precipitate the product. The crystals were collected by filtration and excess amine was removed by washing with 20 mL of diethyl ether. The residue was purified by RP-HPLC using a gradient from water:methanol:triethylamine (90:10:0.5) to methanol:triethylamine (100:0.5). Yields ranged from 38% to 80%.

Method B. The reaction, precipitation, and washing was performed as described for method A. To hydrolyze unreacted *p*-nitrophenylsulfonate, the crystals were stirred in 12.5% aq NH_4OH solution (30 mL) at 60 °C for 20 min. NH_3 was partially removed under reduced pressure until pH 9 was reached. The precipitate was then filtered off and washed with water. The residue was purified by RP-HPLC using a gradient from water:methanol: triethylamine (90:10:0.5) to methanol:triethylamine (100:0.5). Yields ranged from 39% to 62%.

Method C. This method corresponds to method B, but no heating under reflux was applied. The product was isolated in 38% yield.

8-(4-(4-(4-Chlorobenzyl)piperazine-1-sulfonyl)phenyl)-1-propyl-3,7-dihydropurine-2,6-dione (17). ^{1}H NMR (500 MHz, DMSO-d_6) δ 0.88 (t, 3H, J = 7.25 Hz, CH_3), 1.58 (m, 2H, CH_2-CH_3), 2.42 (m (br), 4H, CH_2(piperazinyl)), 2.94 (m (br), 4H, CH_2(piperazinyl)), 3.44 (s, 2H, CH_2(benzyl)), 3.82 (t, 2H, J = 7.25 Hz, N−CH_2(propyl)), 7.23 (d, 2H, J = 8.20 Hz, CH(benzyl)), 7.30 (d, 2H, J = 8.20 Hz, CH(benzyl)), 7.83 (d, 2H, J = 8.15 Hz, CH(phenyl)), 8.32 (d, 2H, J = 8.20 Hz, CH(phenyl)), 11.93 (s (br), 1H, NH), 13.99 (s (br), 1H, NH). ^{13}C NMR (125 MHz, DMSO-d_6) δ 11.32 (CH_3), 21.00 (CH_2−CH_3), 41.62 (N−CH_2(propyl)), 46.10, 51.48 (CH_2(piperazinyl)), 60.48 (CH_2(benzyl)), 108.87 (C-5), 127.07, 128.26, 128.38, 130.60 (CH(phenyl)), 131.65, 133.30, 135.74, 136.94 (C(phenyl)), 147.71 (C-4), 148.17 (C-8), 151.09 (C-2), 155.13 (C-6). LC/ESI-MS: negative mode m/z = 541 ([M − H]$^-$), positive mode m/z = 543 ([M + H]$^+$). Purity (HPLC-UV 254 nm) 99.5%. Anal. ($C_{25}H_{27}ClN_6O_4S\cdot H_2O$) C, H, N.

1-Ethyl-8-(4-(4-(4-trifluoromethylbenzyl)piperazine-1-sulfonyl)phenyl)-3,7-dihydropurine-2,6-dione (24). ^{1}H NMR (500 MHz, DMSO-d_6) δ 1.14 (t, 3H, J = 6.95 Hz, CH_3), 2.45 (m (br), 4H, CH_2(piperazinyl)), 2.95 (m (br), 4H, CH_2(piperazinyl)), 3.55 (s, 2H, CH_2(benzyl)), 3.92 (q, 2H, J = 6.95 Hz, CH_2(ethyl)), 7.45 (d, 2H, J = 7.85 Hz, CH(benzyl)), 7.61 (d, 2H, J = 8.20 Hz, CH(benzyl)), 7.84 (d, 2H, J = 8.50 Hz, CH(phenyl)), 8.33 (d, 2H,

Downloaded by UNIV OF NEWCASTLE on October 11, 2009 | http://pubs.acs.org
Publication Date (Web): May 27, 2009 | doi: 10.1021/jm900413e

J = 8.50 Hz, CH(phenyl)), 11.94 (s (br), 1H, NH), 14.01 (s (br), 1H, NH). ^{13}C NMR (125 MHz, DMSO-d_6) δ 13.35 (CH_3), 35.19 ($\underline{C}H_2-CH_3$), 46.11, 51.58 (CH_2(piperazinyl)), 60.66 (CH_2(benzyl)), 108.83 (C-5), 124.42 (q, J = 270.13 Hz, CF_3), 125.16 (q, J = 3.73 Hz, CH(benzyl)), 127.08 (CH(phenyl)), 127.81 (q, J = 31.48 Hz, $\underline{C}$-CF_3), 128.40 (CH(phenyl)), 129.41 (CH(benzyl)), 133.23, 135.74 (C(phenyl)), 143.00 (C(benzyl)), 147.72 (C-4), 148.09 (C-8), 150.89 (C-2), 154.89 (C-6). LC/ESI-MS: negative mode m/z = 561 ([M − H]$^-$), positive mode m/z = 563 ([M + H]$^+$). Purity (HPLC-UV 254 nm) 96.8%. Anal. ($C_{25}H_{25}F_3N_6O_4S\cdot 0.25H_2O$) C, H, N.

8-(4-(4-(4-Chlorophenyl)piperazine-1-sulfonyl)phenyl)-1-propyl-3,7-dihydropurine-2,6-dione (35). ^{1}H NMR (500 MHz, DMSO-d_6) δ 0.87 (t, 3H, J = 7.25 Hz, CH_3), 1.57 (m, 2H, $C\underline{H}_2-CH_3$), 3.06 (m (br), 4H, CH_2(piperazinyl)), 3.20 (m (br), 4H, CH_2(piperazinyl)), 3.82 (t, 2H, J = 7.25 Hz, N−CH_2(propyl)), 6.90 (d, 2H, J = 8.85 Hz, CH(phenyl)), 7.20 (d, 2H, J = 8.85 Hz, CH(phenyl)), 7.88 (d, 2H, J = 8.50 Hz, CH(phenyl)), 8.34 (d, 2H, J = 8.20 Hz, CH(phenyl)), 11.93 (s (br), 1H, NH), 14.00 (s (br), 1H, NH). ^{13}C NMR (125 MHz, DMSO-d_6) δ 11.31 (CH_3), 20.98 ($\underline{C}H_2-CH_3$), 41.62 (N−CH_2(propyl)), 45.81, 47.91 (CH_2(piperazinyl)), 108.71 (C-5), 117.76 (CH(phenyl)), 123.37 (C(phenyl)), 127.14, 128.44, 128.80 (CH(phenyl)), 133.29, 135.69 (C(phenyl)), 147.73 (C-4), 148.07 (C-8), 149.29 (C(phenyl)), 151.07 (C-2), 155.08 (C-6). LC/ESI-MS: negative mode m/z = 527 ([M − H]$^-$), positive mode m/z = 529 ([M + H]$^+$). Purity (HPLC-UV 254 nm) 99.8%. Anal. ($C_{24}H_{25}ClN_6O_4S\cdot 0.25H_2O$) C, H, N.

Preparation of [^{3}H]35. The labeling reaction was performed by GE Healthcare UK Limited by catalytic hydrogenation of the 1-propargyl-substituted precursor **36** with tritium gas in the presence of Pd/C (10%) using a mixture of ethanol and DMF as solvent. The radioligand [^{3}H]**35** was purified by RP-HPLC. The identity was confirmed by mass spectrometric analysis (see Supporting Information). [^{3}H]**35** displayed a specific activity of 2.70 TBq/mmol (73 Ci/mmol) and a radiochemical purity of 98.9% as determined by HPLC/UV (254 nm).

Fluorimetric Measurement of Intracellular Calcium Concentrations in Jurkat T Cells. Fluorimetric measurements were performed with a FLUOStar Galaxy (BMG Labtech, Offenburg, Germany) at 30 °C. Jurkat T cells were grown in RPMI 1640 medium supplemented with 10% fetal calf serum, 2 mM GlutaMAX (Invitrogen), and 100 IU penicillin and 100 μg/mL streptomycin. The cells were transferred to Falcon tubes, aliquots of cells were counted using a hemocytometer, and the cells were then spun down at 200g and 4 °C for 5 min. After removal of the supernatant, the cells were incubated with Oregon Green BAPTA-1 AM (Invitrogen, 3 μL of a 1 mM solution in DMSO) and with 3 μL of a 25% aq solution of Pluronic F-127) in a final volume of 1 mL of Krebs−Ringer−Hepes (KRH) buffer consisting of NaCl (118.6 mM), KCl (4.7 mM), KH_2PO_4 (1.2 mM), $NaHCO_3$ (4.2 mM), D-glucose (11.7 mM), HEPES (10 mM), $CaCl_2$ (1.3 mM), $MgSO_4$ (1.2 mM), pH 7.4 (with NaOH) in the dark with shaking (600 rpm) at 37 °C for 60 min. Then the cells were washed twice with 1 mL KRH buffer each by centrifugation at 7000 rpm and 4 °C for a few seconds. Then the cells were suspended in fresh KRH buffer and pipetted into 96-well plates at a density of ca. 200000 cells in a volume of 160 μL per well. Before addition of the cells, 20 μL of a solution containing test compound (1-alkyl-8-(piperazine-1-sulfonyl)phenylxanthine derivative) and 3-(3-hydroxypropyl)-7-methyl-8-(*m*-methoxystyryl)-1-propargylxanthine (final concentration: 200 nM) to block A_{2A}AdoR had been added. After 10 min of preincubation and measurement of basic fluorescence levels, 20 μL of a solution containing NECA (10 μM final concentration) was added automatically to each well and changes in fluorescence levels were recorded. The DMSO concentration did not exceed 2.5%. A_{2B} antagonists were tested in 8−10 concentrations spanning at least 3−4 orders of magnitude in order to calculate IC_{50} values. At least three separate experiments were performed each in triplicates or quadruplicates.

Radioligand Binding Assays at A_1, A_{2A} and A_3 Receptors. Membrane preparations and radioligand binding assays at rat A_1 (rat brain cortex), human A_1 (expressed in CHO cells), rat A_{2A} (rat brain striatum), human A_{2A} (expressed in CHO cells), and human A_3 receptors (expressed in CHO cells) were performed as previously described.[59,66,73−75] [^{3}H]2-chloro-N^6-cyclopentyladenosine ([^{3}H]CCPA, 42.6 Ci/mmol, 1 nM), [^{3}H](*E*)-3-(3-hydroxypropyl)-8-(2-(3-methoxyphenyl)vinyl)-7-methyl-1-prop-2-ynyl-3,7-dihydropurine-2,6-dione ([^{3}H]MSX-2, 84 Ci/mmol, 1 nM), and [^{3}H]2-phenyl-8-ethyl-4-methyl-(8*R*)-4,5,7,8-tetrahydro-1*H*-imidazo[2.1-*i*]purin-5-one ([^{3}H]PSB-11, 53 Ci/mmol, 1 nM) were used as A_1, A_{2A}, and A_3 radioligands, respectively.[62−65] The radioligands were custom-labeled by GE Healthcare from suitable precursors as described.[62−65]

Membrane Preparations for A_{2B} Receptor Assays. Membranes of CHO cells expressing the human A_{2B} receptor were prepared by scratching the cells off the previously frozen cell culture dishes in ice-cold hypotonic buffer (5 mM Tris-HCl, 2 mM EDTA, pH 7.4). The cell suspension was homogenized on ice for 20 s with an Ultra-Turrax and spun down for 10 min (4 °C) at 1,000 g. The supernatant was subsequently centrifuged for 60 min at 48000g. The obtained membrane pellets were resuspended in 10 mL of 50 mM Tris-HCl buffer, pH 7.4, and again centrifuged under the same conditions. Then the membrane pellets were resuspended and homogenized in the required amount of 50 mM Tris-HCl puffer, pH 7.4, to obtain a protein concentration of 1−3 mg/mL. Aliquots of the membrane preparation (1 mL each) were stored at −80 C° until used.

A_{2B} Radioligand Binding Assays. Competition experiments with [^{3}H]**35** were performed in a final volume of 500 μL containing 25 μL of test compound dissolved in 50% DMSO/50% Tris-HCl buffer (50 mM, pH 7,4), 275 μL buffer (50 mM Tris-HCl, pH 7,4), 100 μL of radioligand solution in the same buffer (final concentration 0.3 nM), and 100 μL of membrane preparation (30 μg protein per tube in buffer containing adenosine deaminase (2 U/mL, 20 min incubation). Nonspecific binding was determined in the presence of 10 μM 8-cyclopentyl-1,3-dipropylxanthine (DPCPX). After an incubation time of 75 min at rt, the assay mixture was filtered through GF/B glass fiber filters using a Brandel harvester (Brandel, Gaithersburg, MD). Filters were washed four times (3−4 mL each) with ice-cold 50 mM Tris-HCl buffer, pH 7.4, containing 0.1% bovine serum albumin (BSA). Then filters were transferred to vials, incubated for 9 h with 2.5 mL of scintillation cocktail (Beckmann Coulter), and counted in a liquid scintillation counter (Tricarb 2700TR) with a counting efficiency of ∼54%. Three separate experiments were performed in duplicates.

Association studies were performed over a time range of 180 min with 12 different points. Dissociation was initiated by the addition of 10 μM 8-cyclopentyl-1,3-dipropylxanthine after 95 min of preincubation. Two separate experiments were performed in duplicates. The other conditions were as described for competition experiments. Saturation studies were performed over a concentration range of 0.05−1 nM using nine different concentrations of [^{3}H]**35**. All other conditions were as described for competition experiments. Three separate experiments were performed in duplicates. All data were analyzed with GraphPad Prism, Version 4.1 (GraphPad Inc., La Jolla, CA).

Acknowledgment. T.B. was supported by a stipend provided by the Bischöfliche Studienförderung Cusanuswerk. D.C.G.B. was supported by a scholarship of the Deutsche Forschungsgemeinschaft (DFG) within the Graduiertenkolleg GRK 677. W.L. is grateful for a STIBET scholarship by the Deutscher Akademischer Austauschdienst (DAAD).

Supporting Information Available: Elemental analyses of synthesized A_{2B} antagonists; mass spectrum of [^{3}H]PSB-603; experimental data of all synthesized new compounds except **17**, **24**, and **35**. This material is available free of charge via the Internet at http://pubs.acs.org.

References

(1) Fredholm, B. B.; Ijzerman, A. P.; Jacobson, K. A.; Klotz, K. N.; Linden, J. International Union of Pharmacology. XXV. Nomenclature and Classification of Adenosine Receptors. *Pharmacol. Rev* **2001**, *53*, 527–552.

(2) Mann, J. S.; Holgate, S. T.; Renwick, A. G.; Cushley, M. J. Airway effects of purine nucleosides and nucleotides and release with bronchial provocation in asthma. *J. Appl. Physiol.* **1986**, *61*, 1667–1676.

Downloaded by UNIV OF NEWCASTLE on October 11, 2009 | http://pubs.acs.org
Publication Date (Web): May 27, 2009 | doi: 10.1021/jm900413e

Downloaded by UNIV OF NEWCASTLE on October 11, 2009 | http://pubs.acs.org
Publication Date (Web): May 27, 2009 | doi: 10.1021/jm900413e

(3) Huszár, È.; Vass, G.; Vizi, É.; Csoma, Zs.; Barát, E.; Molnár Világos, Gy.; Herjavecz, I.; Horváth, I. Adenosine in exhaled breath condensate in healthy volunteers and in patients with asthma. *Eur. Respir. J.* **2002**, *20*, 1393–1398.
(4) Driver, A. G.; Kukoly, C. A.; Ali, S.; Mustafa, S. J. Adenosine in bronchoalveolar lavage fluid in asthma. *Am. Rev. Respir. Dis.* **1993**, *148*, 91–97.
(5) Blackburn, M. R.; Volmer, J. B.; Thrasher, J. L.; Zhong, H.; Crosby, J. R.; Lee, J. J.; Kellems, R. E. Metabolic consequences of adenosine deaminase deficiency in mice are associated with defects in alveogenesis, pulmonary inflammation, and airway obstruction. *J. Exp. Med.* **2000**, *192*, 159–170.
(6) Chunn, J. L.; Molina, J. G.; Mi, T.; Xia, Y.; Kellems, R. E.; Blackburn, M. R. Adenosine-dependent pulmonary fibrosis in adenosine deaminase-deficient mice. *J. Immunol.* **2005**, *175*, 1937–1946.
(7) Fredholm, B. B.; Irenius, E.; Kull, B.; Schulte, G. Comparison of the potency of adenosine as an agonist at human adenosine receptors expressed in chinese hamster ovary cells. *Biochem. Pharmacol.* **2001**, *61*, 443–448.
(8) Beukers, M. W.; van Oppenraaij, J.; van der Hoorn, P. P.; Blad, C. C.; den Dulk, H.; Brouwer, J.; Ijzerman, A. P. Random mutagenesis of the human adenosine A_{2B} receptor followed by growth selection in yeast. Identification of constitutively active and gain of function mutations. *Mol. Pharmacol.* **2004**, *65*, 702–710.
(9) Feoktistov, I.; Biaggioni, I. Adenosine A_{2B} receptors. *Pharmacol. Rev.* **1997**, *49*, 381–402.
(10) Feoktistov, I.; Goldstein, A. E.; Biaggioni, I. Role of p38 mitogen-activated protein kinase and extracellular signal-regulated protein kinase kinase in adenosine A_{2B} receptor-mediated interleukin-8 production in human mast cells. *Mol. Pharmacol.* **1999**, *55*, 726–734.
(11) Wilson, C. N. Adenosine receptors and asthma in humans. *Br. J. Pharmacol.* **2008**, *155*, 475–486.
(12) Feoktistov, I.; Biaggioni, I. Adenosine A_{2B} receptors evoke interleukin-8 secretion in human mast cells. An enprofylline-sensitive mechanism with implications for asthma. *J. Clin. Invest.* **1995**, *96*, 1979–1986.
(13) Ryzhov, S.; Goldstein, A. E.; Matafonov, A.; Zeng, D.; Biaggioni, I.; Feoktistov, I. Adenosine-activated mast cells induce IgE synthesis by B lymphocytes: an A_{2B}-mediated process involving Th2 cytokines IL-4 and IL-13 with implications for asthma. *J. Immunol.* **2004**, *172*, 7726–7733.
(14) Zhong, H.; Belardinelli, L.; Maa, T.; Feoktistov, I.; Biaggioni, I.; Zeng, D. A_{2B} adenosine receptors increase cytokine release by bronchial smooth muscle cells. *Am. J. Respir. Cell Mol. Biol.* **2004**, *30*, 118–125.
(15) Zhong, H.; Wu, Y.; Belardinelli, L.; Zeng, D. A_{2B} adenosine receptors induce IL-19 from bronchial epithelial cells, resulting in TNF-alpha increase. *Am. J. Respir. Cell Mol. Biol.* **2006**, *35*, 587–592.
(16) Zhong, H.; Belardinelli, L.; Maa, T.; Zeng, D. Synergy between A_{2B} adenosine receptors and hypoxia in activating human lung fibroblasts. *Am. J. Respir. Cell Mol. Biol.* **2005**, *32*, 2–8.
(17) Linden, J. New insights into the regulation of inflammation by adenosine. *J. Clin. Invest.* **2006**, *116*, 1835–1837.
(18) Phan, S. H. The myofibroblast in pulmonary fibrosis. *Chest* **2002**, *122*, 286–289.
(19) Ryzhov, S.; Zaynagetdinov, R.; Goldstein, A. E.; Novitskiy, S. V.; Dikov, M. M.; Blackburn, M. R.; Biaggioni, I.; Feoktistov, I. Effect of A_{2B} adenosine receptor gene ablation on proinflammatory adenosine signaling in mast cells. *J. Immunol.* **2008**, *180*, 7212–7220.
(20) Kreckler, L. M.; Wan, T. C.; Ge, Z. D.; Auchampach, J. A. Adenosine inhibits tumor necrosis factor-alpha release from mouse peritoneal macrophages via A_{2A} and A_{2B} but not the A_3 adenosine receptor. *J. Pharmacol. Exp. Ther.* **2006**, *317*, 172–180.
(21) Yang, D.; Zhang, Y.; Nguyen, H. G.; Koupenova, M.; Chauhan, A. K.; Makitalo, M.; Jones, M. R.; St. Hilaire, C.; Seldin, D. C.; Toselli, P.; Lamperti, E.; Schreiber, B. M.; Gavras, H.; Wagner, D. D.; Ravid, K. The A_{2B} adenosine receptor protects against inflammation and excessive vascular adhesion. *J. Clin. Invest.* **2006**, *116*, 1913–1923.
(22) Ryzhov, S.; Zaynagetdinov, R.; Goldstein, A. E.; Novitskiy, S. V.; Blackburn, M. R.; Biaggioni, I.; Feoktistov, I. Effect of A_{2B} adenosine receptor gene ablation on adenosine-dependent regulation of proinflammatory cytokines. *J. Pharmacol. Exp. Ther.* **2008**, *324*, 694–700.
(23) Hasko, G.; Kuhel, D. G.; Chen, J. F.; Schwarzschild, M. A.; Deitch, E. A.; Mabley, J. G.; Marton, A.; Szabo, C. Adenosine inhibits IL-12 and TNF-[alpha] production via adenosine A_{2a} receptor-dependent and independent mechanisms. *FASEB J.* **2000**, *14*, 2065–2074.
(24) Hasko, G.; Cronstein, B. N. Adenosine: an endogenous regulator of innate immunity. *Trends Immunol.* **2004**, *25*, 33–39.
(25) Sun, C. X.; Zhong, H.; Mohsenin, A.; Morschl, E.; Chunn, J. L.; Molina, J. G.; Belardinelli, L.; Zeng, D.; Blackburn, M. R. Role of A_{2B} adenosine receptor signaling in adenosine-dependent pulmonary inflammation and injury. *J. Clin. Invest.* **2006**, *116*, 2173–2182.
(26) Mustafa, S. J.; Nadeem, A.; Fan, M.; Zhong, H.; Belardinelli, L.; Zeng, D. Effect of a specific and selective A_{2B} adenosine receptor antagonist on adenosine agonist AMP and allergen-induced airway responsiveness and cellular influx in a mouse model of asthma. *J. Pharmacol. Exp. Ther.* **2007**, *320*, 1246–1251.
(27) Elzein, E.; Kalla, R. V.; Li, X.; Perry, T.; Gimbel, A.; Zeng, D.; Lustig, D.; Leung, K.; Zablocki, J. Discovery of a novel A_{2B} adenosine receptor antagonist as a clinical candidate for chronic inflammatory airway diseases. *J. Med. Chem.* **2008**, *51*, 2267–2278.
(28) Holgate, S. T. The identification of the adenosine A_{2B} receptor as a novel therapeutic target in asthma. *Br. J. Pharmacol.* **2005**, *145*, 1009–1015.
(29) Abo-Salem, O. M.; Hayallah, A. M.; Bilkei-Gorzo, A.; Filipek, B.; Zimmer, A.; Müller, C. E. Antinociceptive effects of novel A_{2B} adenosine receptor antagonists. *J. Pharmacol. Exp. Ther.* **2004**, *308*, 358–366.
(30) Bilkei-Gorzo, A.; Abo-Salem, O. M.; Hayallah, A. M.; Michel, K.; Müller, C. E.; Zimmer, A. Adenosine receptor subtype-selective antagonists in inflammation and hyperalgesia. *Naunyn-Schmiedeberg's Arch. Pharmacol.* **2008**, *377*, 65–76.
(31) Strohmeier, G. R.; Reppert, S. M.; Lencer, W. I.; Madara, J. L. The A_{2B} adenosine receptor mediates cAMP responses to adenosine receptor agonists in human intestinal epithelia. *J. Biol. Chem.* **1995**, *270*, 2387–2394.
(32) Sitaraman, S. V.; Merlin, D.; Wang, L.; Wong, M.; Gewirtz, A. T.; Si-Tahar, M.; Madara, J. L. Neutrophil−epithelial crosstalk at the intestinal lumenal surface mediated by reciprocal secretion of adenosine and IL-6. *J. Clin. Invest.* **2001**, *107*, 861–869.
(33) Kolachala, V.; Asamoah, V.; Wang, L.; Obertone, T. S.; Ziegler, T. R.; Merlin, D.; Sitaraman, S. V. TNF-alpha upregulates adenosine 2b (A2b) receptor expression and signaling in intestinal epithelial cells: a basis for A2bR overexpression in colitis. *Cell. Mol. Life Sci.* **2005**, *62*, 2647–2657.
(34) Kolachala, V. L.; Vijay-Kumar, M.; Dalmasso, G.; Yang, D.; Linden, J.; Wang, L.; Gewirtz, A.; Ravid, K.; Merlin, D.; Sitaraman, S. V. A_{2B} adenosine receptor gene deletion attenuates murine colitis. *Gastroenterology* **2008**, *135*, 861–870.
(35) Kolachala, V.; Ruble, B.; Vijay-Kumar, M.; Wang, L.; Mwangi, S.; Figler, H.; Figler, R.; Srinivasan, S.; Gewirtz, A.; Linden, J.; Merlin, D.; Sitaraman, S. V. Blockade of adenosine A_{2B} receptors ameliorates murine colitis. *Br. J. Pharmacol.* **2008**, *155*, 127–137.
(36) Kolachala, V. L.; Bajaj, R.; Chalasani, M.; Sitaraman, S. V. Purinergic receptors in gastrointestinal inflammation. *Am. J. Physiol. Gastrointest. Liver Physiol.* **2008**, *294*, G401–410.
(37) Fiebich, B. L.; Biber, K.; Gyufko, K.; Berger, M.; Bauer, J.; van Calker, D. Adenosine A_{2b} receptors mediate an increase in interleukin (IL)-6 mRNA and IL-6 protein synthesis in human astroglioma cells. *J. Neurochem.* **1996**, *66*, 1426–1431.
(38) Trincavelli, M. L.; Marroni, M.; Tuscano, D.; Ceruti, S.; Mazzola, A.; Mitro, N.; Abbracchio, M. P.; Martini, C. Regulation of A_{2B} adenosine receptor functioning by tumour necrosis factor a in human astroglial cells. *J. Neurochem.* **2004**, *91*, 1180–1190.
(39) Ryzhov, S.; Novitskiy, S. V.; Zaynagetdinov, R.; Goldstein, A. E.; Carbone, D. P.; Biaggioni, I.; Dikov, M. M.; Feoktistov, I. Host A(2B) adenosine receptors promote carcinoma growth. *Neoplasia* **2008**, *10*, 987–995.
(40) Linden, J.; Thai, T.; Figler, H.; Jin, X.; Robeva, A. S. Characterization of human A_{2B} adenosine receptors: radioligand binding, western blotting, and coupling to G(q) in human embryonic kidney 293 cells and HMC-1 mast cells. *Mol. Pharmacol.* **1999**, *56*, 705–713.
(41) Hayallah, A. M.; Sandoval-Ramirez, J.; Reith, U.; Schobert, U.; Preiss, B.; Schumacher, B.; Daly, J. W.; Müller, C. E. 1,8-Disubstituted xanthine derivatives: synthesis of potent A_{2B}-selective adenosine receptor antagonists. *J. Med. Chem.* **2002**, *45*, 1500–1510.
(42) Yan, L.; Bertarelli, D. C.; Hayallah, A. M.; Meyer, H.; Klotz, K. N.; Müller, C. E. A new synthesis of sulfonamides by aminolysis of *p*-nitrophenylsulfonates yielding potent and selective adenosine A_{2B} receptor antagonists. *J. Med. Chem.* **2006**, *49*, 4384–4391.
(43) Kim, Y. C.; Ji, X.; Melman, N.; Linden, J.; Jacobson, K. A. Anilide derivatives of an 8-phenylxanthine carboxylic congener are highly potent and selective antagonists at human A(2B) adenosine receptors. *J. Med. Chem.* **2000**, *43*, 1165–1172.
(44) Baraldi, P. G.; Tabrizi, M. A.; Preti, D.; Bovero, A.; Romagnoli, R.; Fruttarolo, F.; Zaid, N. A.; Moorman, A. R.; Varani, K.; Gessi, S.; Merighi, S.; Borea, P. A. Design, synthesis, and biological evaluation of new 8-heterocyclic xanthine derivatives as highly potent and selective human A_{2B} adenosine receptor antagonists. *J. Med. Chem.* **2004**, *47*, 1434–1447.
(45) Stefanachi, A.; Brea, J. M.; Cadavid, M. I.; Centeno, N. B.; Esteve, C.; Loza, M. I.; Martinez, A.; Nieto, R.; Ravina, E.; Sanz, F.; Segarra, V.; Sotelo, E.; Vidal, B.; Carotti, A. 1-, 3-, and 8-Substituted-9-deazaxanthines as potent and selective antagonists at the human A_{2B} adenosine receptor. *Bioorg. Med. Chem.* **2008**, *16*, 2852–2869.
(46) Castelhano, A. L.; McKibben, B.; Steinig, A. G. Pyrrolopyrimidine A_{2B} selective antagonist compounds, their synthesis and use. Patent WO Patent 2003053361, 2003.

(47) Beukers, M. W.; Meurs, I.; Ijzerman, A. P. Structure−affinity relationships of adenosine A_{2B} receptor ligands. *Med. Res. Rev.* **2006**, *26*, 667–698.
(48) Kiec-Kononowicz, K.; Drabczynska, A.; Pekala, E.; Michalak, B.; Müller, C. E.; Schumacher, B.; Karolak-Wojciechowska, J.; Duddeck, H.; Rockitt, S.; Wartchow, R. New developments in A_1 and A_2 adenosine receptor antagonists. *Pure Appl. Chem.* **2001**, *73*, 1411–1420.
(49) Baraldi, P. G.; Tabrizi, M. A.; Gessi, S.; Borea, P. A. Adenosine receptor antagonists: Translating medicinal chemistry and pharmacology into clinical utility. *Chem. Rev.* **2008**, *108*, 238–263.
(50) Auchampach, J. A.; Kreckler, L. M.; Wan, T. C.; Maas, J. E.; van der Hoeven, D.; Gizewski, E.; Narayanan, J.; Maas, G. E. Characterization of the A_{2B} adenosine receptor from mouse, rabbit, and dog. *J. Pharmacol. Exp. Ther.* **2009**, *329*, 2−13.
(51) Kim, S. A.; Marshall, M. A.; Melman, N.; Kim, H. S.; Müller, C. E.; Linden, J.; Jacobson, K. A. Structure−activity relationships at human and rat A_{2B} adenosine receptors of xanthine derivatives substituted at the 1-, 3-, 7-, and 8-positions. *J. Med. Chem.* **2002**, *45*, 2131–2138.
(52) Bertarelli, D. C.; Diekmann, M.; Hayallah, A. M.; Rüsing, D.; Iqbal, J.; Preiss, B.; Verspohl, E. J.; Müller, C. E. Characterization of human and rodent native and recombinant adenosine A_{2B} receptors by radioligand binding studies. *Purinergic Signal.* **2006**, *2*, 559–571.
(53) Ji, X. D.; Kim, Y. C.; Ahern, D. G.; Linden, J.; Jacobson, K. A. [^{3}H]MRS 1754, a selective antagonist radioligand for A_{2B} adenosine receptors. *Biochem. Pharmacol.* **2001**, *61*, 657–663.
(54) Baraldi, P. G.; Tabrizi, M. A.; Preti, D.; Bovero, A.; Fruttarolo, F.; Romagnoli, R.; Moorman, A. R.; Gessi, S.; Merighi, S.; Varani, K.; Borea, P. A. [^{3}H]-MRE 2029-F20, a selective antagonist radioligand for the human A_{2B} adenosine receptors. *Bioorg. Med. Chem. Lett.* **2004**, *14*, 3607–3610.
(55) Steward, M.; Steinig, A. G.; Ma, C.; Song, J. P.; McKibben, B.; Castelhano, A. L.; MacLennan, S. J. [^{3}H]OSIP339391, a selective, novel, and high affinity antagonist radioligand for adenosine A_{2B} receptors. *Biochem. Pharmacol.* **2004**, *68*, 305–312.
(56) Müller, C. E. Synthesis of 3-substituted 6-aminouracils. *Tetrahedron Lett.* **1991**, *32*, 6539–6540.
(57) Müller, C. E. General synthesis and properties of 1-monosubstituted xanthines. *Synthesis* **1993**, *1*, 125–128.
(58) Müller, C. E.; Sandoval-Ramirez, J. A new versatile synthesis of xanthines with variable substituents in the 1-, 3-, 7-, and 8-positions. *Synthesis* **1995**, *10*, 1295–1299.
(59) Yan, L.; Müller, C. E. Preparation, properties, reactions, and adenosine receptor affinities of sulfophenylxanthine nitrophenyl esters: toward the development of sulfonic acid prodrugs with peroral bioavailability. *J. Med. Chem.* **2004**, *47*, 1031–1043.
(60) Müller, C. E. Formation of oxazolo[3,2-*a*]purinones from propynyluracils. *J. Org. Chem.* **1994**, *59*, 1928–1929.
(61) Hockemeyer, J.; Burbiel, J. C.; Müller, C. E. Multigram-scale syntheses, stability, and photoreactions of A_{2A} adenosine receptor antagonists with 8-styrylxanthine structure: potential drugs for Parkinson's disease. *J. Org. Chem.* **2004**, *69*, 3308–3318.
(62) Bulicz, J.; Bertarelli, D. C.; Baumert, D.; Fülle, F.; Müller, C. E.; Heber, D. Synthesis and pharmacology of pyrido[2,3-*d*]pyrimidinediones bearing polar substituents as adenosine receptor antagonists. *Bioorg. Med. Chem.* **2006**, *14*, 2837–2849.
(63) Klotz, K. N.; Lohse, M. J.; Schwabe, U.; Cristalli, G.; Vittori, S.; Grifantini, M. 2-Chloro-N^6-[^{3}H]cyclopentyladenosine ([^{3}H]CCPA)—a high affinity agonist radioligand for A_1 adenosine receptors. *Naunyn-Schmiedeberg's Arch. Pharmacol.* **1989**, *340*, 679–683.
(64) Müller, C. E.; Maurinsh, J.; Sauer, R. Binding of [^{3}H]MSX-2 (3-(3-hydroxypropyl)-7-methyl-8-(*m*-methoxystyryl)-1-propargylxanthine) to rat striatal membranes—a new, selective antagonist radioligand for A_{2A} adenosine receptors. *Eur. J. Pharm. Sci.* **2000**, *10*, 259–265.
(65) Müller, C. E.; Diekmann, M.; Thorand, M.; Ozola, V. [^{3}H]8-Ethyl-4-methyl-2-phenyl-(8*R*)-4,5,7,8-tetrahydro-1*H*-imidazo[2,1-*i*]-purin-5-one ([^{3}H]PSB-11), a novel high-affinity antagonist radioligand for human A_3 adenosine receptors. *Bioorg. Med. Chem. Lett.* **2002**, *12*, 501–503.
(66) Klotz, K. N.; Hessling, J.; Hegler, J.; Owman, C.; Kull, B.; Fredholm, B. B.; Lohse, M. J. Comparative pharmacology of human adenosine receptor subtypes—characterization of stably transfected receptors in CHO cells. *Naunyn-Schmiedeberg's Arch. Pharmacol.* **1998**, *57*, 1–9.
(67) Mirabet, M.; Mallol, J.; Lluis, C.; Franco, R. Calcium mobilization in Jurkat cells via A_{2B} adenosine receptors. *Br. J. Pharmacol.* **1997**, *122*, 1075–1082.
(68) Sauer, R.; Maurinsh, J.; Reith, U.; Fülle, F.; Klotz, K. N.; Müller, C. E. Water-soluble phosphate prodrugs of 1-propargyl-8-styrylxanthine derivatives, A_{2A}-selective adenosine receptor antagonists. *J. Med. Chem.* **2000**, *43*, 440–448.
(69) Gessi, S.; Varani, K.; Merighi, S.; Cattabriga, E.; Pancaldi, C.; Szabadkai, Y.; Rizzuto, R.; Klotz, K. N.; Leung, E.; Mac Lennan, S.; Baraldi, P. G.; Borea, P. A. Expression, pharmacological profile, and functional coupling of A_{2B} receptors in a recombinant system and in peripheral blood cells using a novel selective antagonist radioligand, [^{3}H]MRE 2029-F20. *Mol. Pharmacol.* **2005**, *67*, 2137–2147.
(70) Ji, X. D.; Jacobson, K. A. Use of the triazolotriazine [^{3}H]ZM 241385 as a radioligand at recombinant human A_{2B} adenosine receptors. *Drug Des. Discovery* **1999**, *16*, 217–226.
(71) Clark, D. E. Rapid calculation of polar molecular surface area and its application to the prediction of transport phenomena. 1. Prediction of intestinal absorption. *J. Pharm. Sci.* **1999**, *88*, 807–814.
(72) Lipinski, C. A.; Lombardo, F.; Dominy, B. W.; Feeney, P. J. Experimental and computational approaches to estimate solubility and permeability in drug discovery and development settings. *Adv. Drug Delivery Rev.* **2001**, *46*, 3–26.
(73) Weyler, S.; Fülle, F.; Diekmann, M.; Schumacher, B.; Hinz, S.; Klotz, K. N.; Müller, C. E. Improving potency, selectivity, and water solubility of adenosine A_1 receptor antagonists: xanthines modified at position 3 and related pyrimido[1,2,3-*cd*]purinediones. *ChemMedChem* **2006**, *1*, 891–902.
(74) Drabczynska, A.; Müller, C. E.; Schiedel, A.; Schumacher, B.; Karolak-Wojciechowska, J.; Fruzinski, A.; Zobnina, W.; Yuzlenko, O.; Kiec-Kononowicz, K. Phenylethyl-substituted pyrimido[2,1-*f*]purinediones and related compounds: structure−activity relationships as adenosine A_1 and A_{2A} receptor ligands. *Bioorg. Med. Chem.* **2007**, *15*, 6956–6974.
(75) Drabczynska, A.; Müller, C. E.; Karolak-Wojciechowska, J.; Schumacher, B.; Schiedel, A.; Yuzlenko, O.; Kiec-Kononowicz, K. N^9-Benzyl-substituted 1,3-dimethyl- and 1,3-dipropyl-pyrimido[2,1-*f*]purinediones: synthesis and structure−activity relationships at adenosine A_1 and A_{2A} receptors. *Bioorg. Med. Chem.* **2007**, *15*, 5003–5017.

JM900413E

Downloaded by UNIV OF NEWCASTLE on October 11, 2009 | http://pubs.acs.org
Publication Date (Web): May 27, 2009 | doi: 10.1021/jm900413e